HHS Public Access

Author manuscript

Cell Rep. Author manuscript; available in PMC 2024 February 16.

Published in final edited form as:

Cell Rep. 2023 October 31; 42(10): 113157. doi:10.1016/j.celrep.2023.113157.

Hyperpolarization-activated cyclic nucleotide-gated cation channel 3 promotes HCC development in a female-biased manner

Yueqi Zhang[1,2], **Xinhui Liu**[1,3], **Kairui Sun**[1,4], **Yue Luo**[1,3], **Jack Yang**[1], **Aimin Li**[1,3], **Matti Kiupel**[5], **Stefanie Fenske**[6], **Martin Biel**[6], **Qing-Sheng Mi**[7,8], **Hongbing Wang**[1], **Hua Xiao**[1,2,9,*]

[1]Department of Physiology, Michigan State University, East Lansing, MI 48824, USA

[2]Cell and Molecular Biology Program, Michigan State University, East Lansing, MI 48824, USA

[3]Cancer Center, Southern Medical University, Guangzhou, Guangdong 510315, China

[4]College of Osteopathic Medicine, Michigan State University, East Lansing, MI 48824, USA

[5]Department of Pathobiology and Diagnostic Investigation, Michigan State University, East Lansing, MI 48824, USA

[6]Department of Pharmacy – Center for Drug Research, Ludwig-Maximilians Universität München, 81377 München, Germany

[7]Immunology Program, Henry Ford Cancer Institute, Henry Ford Health, Detroit, MI 48202, USA

[8]Center for Cutaneous Biology and Immunology, Department of Dermatology, Henry Ford Health, Detroit, MI 48202, USA

[9]Lead contact

SUMMARY

Sex differences in hepatocellular carcinoma (HCC) development are regulated by sex and non-sex chromosomes, sex hormones, and environmental factors. We previously reported that *Ncoa5*$^{+/-}$ mice develop HCC in a male-biased manner. Here we show that NCOA5 expression is reduced in male patient HCCs while the expression of an NCOA5-interacting tumor suppressor, *TIP30*, is lower in female HCCs. *Tip30* heterozygous deletion does not change HCC incidence in *Ncoa5*$^{+/-}$ male mice but dramatically increases HCC incidence in *Ncoa5*$^{+/-}$ female mice, accompanied by hepatic hyperpolarization-activated cyclic nucleotide-gated cation channel 3

*Correspondence: xiaoh@msu.edu.

AUTHOR CONTRIBUTIONS

Conceptualization, H.X., Y.Z., H.W., and Q.-S.M.; data curation, Y.Z., X.L., K.S., Y.L., A.L., and H.X.; formal analysis, Y.Z., X.L., M.K., and H.X.; funding acquisition, H.X.; investigation, Y.Z., X.L., K.S., Y.L., J.Y., A.L., M.K., S.F., M.B., and H.X.; methodology, H.X., Y.Z., and X.L.; project administration, H.X.; resources, H.X., H.W., Q.-S.M., S.F., and M.B.; software, Y.Z.; supervision: H.X.; validation, Y.Z., X.L., K.S., Y.L., J.Y., M.K., and H.X.; visualization, Y.Z., H.X., and X.L.; writing – original draft, H.X. and Y.Z.; writing – review & editing, all authors.

DECLARATION OF INTERESTS

The authors declare no competing interests.

SUPPLEMENTAL INFORMATION

Supplemental information can be found online at https://doi.org/10.1016/j.celrep.2023.113157.

(HCN3) overexpression. HCN3 overexpression cooperates with MYC to promote mouse HCC development, whereas *Hcn3* knockout preferentially hinders HCC development in female mice. Furthermore, HCN3 amplification and overexpression occur in human HCCs and correlate with a poorer prognosis of patients in a female-biased manner. Our results suggest that TIP30 and NCOA5 protect against female liver oncogenesis and that HCN3 is a female-biased HCC driver.

In brief

Zhang et al. report a female-biased mechanism underlying hepatocellular carcinoma (HCC) development that is regulated by transcription coregulators NCOA5 and TIP30. The ion channel HCN3 is identified as a female-biased HCC driver.

Graphical abstract

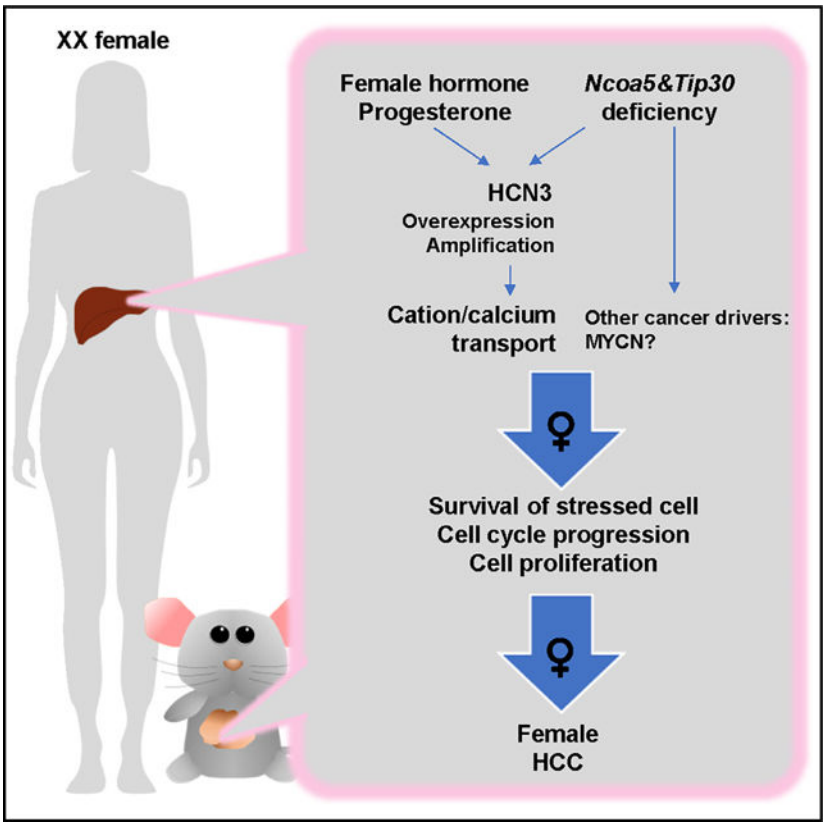

INTRODUCTION

Liver cancer is the ninth most common cancer in women and the fifth most common in men in the United States, and is the third leading cause of cancer death worldwide. Despite the decline in incidence and mortality rates of most cancer types over the last decade, liver cancer incidence and mortality have steadily increased in the United States.[1,2] Notably, liver cancer incidence and mortality rates have risen faster in women than in men.[2,3] Hepatocellular carcinoma (HCC) is the most common type of primary liver cancer, and its incidence in men is two to four times higher than in women.[4] A similar male predominance

of liver tumor development has also been observed in rodent models of HCC.[5–8] Previous studies have suggested that sex differences in HCC risk can be partly attributed to sex disparities in environmental exposures such as hepatitis B virus (HBV) infection and alcohol consumption.[9–12] However, a recent prospective cohort analysis on cancer risk for 21 cancer types, including HCC, suggests that genetic and epigenetic differences between men and women affect susceptibility to cancer and that environmental exposures alone may only explain some of the sex disparities in cancer.[13] Thus, understanding the molecular mechanisms underlying sex differences in HCC development will improve prevention, treatment, and outcomes for male and female patients with HCC.

HCC has the most significant sex differences in autosomal mutational profiles among cancers of non-reproductive tissues among 18 tumor types examined,[14] suggesting etiological differences between male and female HCC. There is growing evidence of sex-biased mechanisms driving HCC initiation and progression in males and females,[15–17] which are influenced by hormones and lifestyle.[18–20] The β-catenin encoded by *CTNNB1*, a well-known liver cancer driver, is a male-biased HCC driver with a higher mutation frequency in male HCC specimens. *CTNNB1* mutations also affect patient outcomes in both sexes but have a male-biased preference [14]. Identifying sex-biased liver cancer drivers may allow us to discover new opportunities for developing sex-specific anti-HCC therapies. Although extensive studies on hepatocarcinogenesis have uncovered protective or promotive mechanisms related to sex hormones[18,21] and non-sex hormone factors,[22,23] most studies have primarily used male subjects because of the prevalence of HCC in males, resulting in a female patient and animal under-representation. Consequently, those identified sex-biased liver cancer drivers tend to promote cancer development in a male-biased manner. Recently, several female-preferentially expressed factors such as miR26s and CYP39A1 have been reported to suppress HCC development.[24–26] Furthermore, four genes with a higher mutation frequency in female HCCs were identified in HBV-related and aflatoxin-exposed HCC patients.[27] However, none of these genes have been reported as HCC drivers for promoting malignant transformation, and the mechanisms driving HCC development in females remain poorly understood.

Nuclear receptor coactivator 5 (NCOA5) is a unique nuclear receptor coactivator with both coactivator and corepressor functions. It cooperates with Tat-interacting protein 30 (TIP30), a known tumor suppressor,[28,29] to repress estrogen receptor α (ERα)-activated c-myc gene transcription in estrogen-dependent and independent ways.[30] NCOA5 plays a critical role in the sex differences in HCC development, as its haploinsufficiency leads to spontaneous HCC development in a male-biased manner through increased pro-inflammatory cytokine expression, p53-p21 pathway activation, and populations of immunosuppressive cells.[8,31–33] To investigate the mechanism preventing HCC development in female *Ncoa5*$^{+/-}$ mice, we generated mice carrying dual *Ncoa5* and *Tip30* heterozygous deletions for genetic and biochemical analyses. Our results demonstrate that TIP30 is critical in suppressing HCC development in *Ncoa5*$^{+/-}$ female mice and that hyperpolarization-activated cyclic nucleotide-gated cation channel 3 (HCN3), whose expression is significantly increased in the livers of *Ncoa5*$^{+/-}$*Tip30*$^{+/-}$ females, is a female-biased cancer driver for promoting HCC development.

RESULTS

NCOA5 and TIP30 are differentially expressed in male and female HCCs and are inter-related in expression levels

We previously reported that NCOA5 haploinsufficiency resulted in a high incidence of HCC in aged male mice but rarely in female mice.[8] To explore whether there are sex-different roles of NCOA5 in human hepatocarcinogenesis, we first determined the levels of NCOA5 expression in HCCs from male and female patients of the TCGA (The Cancer Genome Atlas) cohort. We found that HCC specimens from male patients had significantly lower *NCOA5* mRNA than female patients (Figures 1A and 1B). Through protein-protein interaction networks, we identified NCOA5-interacting proteins with different expression levels between HCCs from male and female patients (Figure S1A). One of these proteins is TIP30 (HTATIP2) that can cooperate with NCOA5 to regulate ERa-mediated c-*myc* gene transcription.[30] TIP30 mRNA levels in HCCs from female patients were significantly lower compared to HCCs from male patients (Figure 1B). Intriguingly, the mRNA levels of *NCOA5* and *TIP30* negatively correlated with each other in HCCs from the TCGA cohort (Figure 1C). This negative correlation was also observed in younger female and older male and female mice, as *Tip30* mRNA levels were increased in the livers of 2- and 5-month-old *Ncoa5*$^{+/-}$ female mice but not in age-matched *Ncoa5*$^{+/-}$ male mice (Figure 1D). In contrast, *Tip30* mRNA levels were increased in the livers of *Ncoa5*$^{+/-}$ male mice at an older age (Figure 1E). These results indicate that NCOA5 and TIP30 expressions are sex dependent and inter-related in both mouse and human livers. Given its tumor-suppressive role,[29] we hypothesize that *Tip30* is critical in suppressing hepatocarcinogenesis in females with NCOA5 deficiency.

Tip30 heterozygous deletion promoted the HCC development of *Ncoa5*-deficient mice in a female-biased manner

To test the aforestated hypothesis, we sought to determine whether the downregulation of TIP30 increases liver tumor incidence in the *Ncoa5*$^{+/-}$ mouse model of HCC. Since a high incidence of lung and mammary gland tumors in *Tip30*$^{-/-}$ mice[28,34] might complicate the results, we monitored liver tumor development in a cohort of wild-type, *Tip30*$^{+/-}$, *Ncoa5*$^{+/-}$, and *Ncoa5*$^{+/-}$*Tip30*$^{+/-}$ female and male mice. Mice were euthanized and subjected to complete necropsy when moribund or at the age of 18 months. Liver, lung, and mammary tumors were detected at the surface of the organs in mice older than 10 months. Interestingly, a liver tumor incidence of 80% was observed in *Ncoa5*$^{+/-}$*Tip30*$^{+/-}$ female mice, whereas only 10% of *Ncoa5*$^{+/-}$ female mice developed liver tumors. No liver tumor was detected in wild-type or *Tip30*$^{+/-}$ female mice (Figure 2A). In contrast, liver tumor incidence was not increased in *Ncoa5*$^{+/-}$*Tip30*$^{+/-}$ male mice compared to *Ncoa5*$^{+/-}$ male mice (Figure 2A). Among *Tip30*$^{+/-}$ female mice, 26.7% developed lung tumors and 13.3% developed mammary gland tumors. Among *Ncoa5*$^{+/-}$*Tip30*$^{+/-}$ female mice, 10% developed lung tumors and another 10% developed mammary gland tumors without comorbidities with liver tumors. No lung or mammary gland tumors were observed in *Ncoa5*$^{+/-}$ female mice. All liver tumors from female and male *Ncoa5*$^{+/-}$*Tip30*$^{+/-}$ mice were well to moderately differentiated HCCs with similar histological features (Figure 2B), and the livers of 10-month-old *Ncoa5*$^{+/-}$*Tip30*$^{+/-}$ female mice displayed moderate to severe steatosis compared

to the livers of age-matched *Ncoa5*$^{+/-}$ female mice (Figure S1B), similar to those previously described in *Ncoa5*$^{+/-}$ male mice.[8] Heterozygous deletion of *Tip30* alone did not result in any case of HCC, nor did it change the liver histology significantly in female mice (Figures 2C and S1C). Notably, heterozygous deletion of *Ncoa5* resulted in moderately disrupted liver architecture and vacuolated hepatocytes in aged female mice (Figures 2C and S1C), even though the severities were much less compared to that in age-matched male mice. In line with these results, both a-fetoprotein (AFP) levels and alanine aminotransferase (ALT) activity were significantly increased in the serum of *Ncoa5*$^{+/-}$ *Tip30*$^{+/-}$ female mice at the age of 18 months compared to age-matched female mice in other genotypical groups, confirming the severe liver damage and liver malignancy in dual-mutant female mice (Figure 2D). ALT activity was also increased in the serum of 18-month-old *Ncoa5*$^{+/-}$ female mice compared to wild-type mice (Figure 2D). Immunohistochemical (IHC) staining of macrophage marker Mac-2 revealed increased macrophage infiltration to the livers of 18-month-old *Ncoa5*$^{+/-}$ *Tip30*$^{+/-}$ female mice compared to *Ncoa5*$^{+/-}$ or wild-type age-matched female mice (Figure 2E). Together, these data demonstrated that heterozygous *Tip30* deletion preferentially promotes HCC development in *Ncoa5*$^{+/-}$ female mice.

Deletion of *Tip30* in *Ncoa5*$^{+/-}$ female mice upregulated pathways in cation transport and cell cycle and HCN3 expression

To identify genes and signal pathways that promote the hepatocarcinogenesis in *Ncoa5*$^{+/-}$ *Tip30*$^{+/-}$ female mice, we performed RNA sequencing and transcriptome analysis on isolated RNA from the livers of 5-month-old wild-type, *Ncoa5*$^{+/-}$, *Tip30*$^{+/-}$, and *Ncoa5*$^{+/-}$ *Tip30*$^{+/-}$ female mice. Gene ontology (GO) enrichment analysis revealed that the top five GO.bp pathways uniquely upregulated in *Ncoa5*$^{+/-}$ *Tip30*$^{+/-}$ female livers included cycle G_2/M phase transitions and multiple pathways related to the regulation of transport of calcium and other cations (Figure 3A). The bile acid metabolism and vesicle transport associated with the endoplasmic reticulum (ER) and Golgi apparatus were uniquely downregulated in the livers of *Ncoa5*$^{+/-}$ *Tip30*$^{+/-}$ female mice. Unexpectedly, *Tip30* deletion did not further activate inflammatory pathways that were upregulated in *Ncoa5*$^{+/-}$ female mouse livers, nor did it further activate p53-p21 signaling pathways (Figure S2). Consistently, the mRNA levels of interleukin-6 (IL-6) and tumor necrosis factor α were not increased in the livers of 5-month-old *Ncoa5*$^{+/-}$ *Tip30*$^{+/-}$ female mice compared to age-matched *Ncoa5*$^{+/-}$ or *Tip30*$^{+/-}$ female mice, nor were they raised in the HCCs or adjacent normal liver tissues of 18-month-old *Ncoa5*$^{+/-}$ *Tip30*$^{+/-}$ female mice compared to *Ncoa5*$^{+/-}$ female mice (Figures S3A and S3B). IHC staining and ELISA confirmed no increased IL-6-expressing cells and protein levels in the livers of 18-month-old *Ncoa5*$^{+/-}$ *Tip30*$^{+/-}$ female mice compared to those of *Ncoa5*$^{+/-}$ female mice (Figures S3C and S3D). Next, we analyzed the differentially expressed genes (DEGs) between wild-type and three types of mutant livers (adjusted $p < 0.05$). Dual *Ncoa5* and *Tip30* heterozygous deletions resulted in the highest number of DEGs (1,099), while *Ncoa5* heterozygous deletion alone significantly changed the expression of 250 genes, and *Tip30* heterozygous deletion alone significantly changed the expression of only 43 genes (Figure 3B). Only two DEGs, upregulated *Hcn3*, encoding a cation channel known to mediate the transport of potassium, sodium, and calcium,[37,38] and downregulated *Wnt5a*, are shared by all three mutant liver groups (Figures 3B and S3E). Notably, the proto-oncogene *Mycn* was significantly upregulated only in the

dual-mutant livers (Figures 3B and S3F). When comparing gene expression profiles between livers of *Ncoa5*$^{+/-}$ *Tip30*$^{+/-}$ and *Ncoa5*$^{+/-}$ female mice, the most significantly upregulated protein-coding genes in livers of *Ncoa5*$^{+/-}$ *Tip30*$^{+/-}$ female mice was *Hcn3* (Figure 3C). Moreover, the dual heterozygous deletions did not increase *Hcn3* mRNA in the livers of male mice (Figure 3D). In wild-type mice, liver *Hcn3* mRNA levels were higher in females than in males (Figure 3E). Protein expression of HCN3 was also increased in the livers of *Ncoa5*$^{+/-}$ *Tip30*$^{+/-}$ female mice (Figures 3F and S3G). Collectively, these results suggest that hepatic HCN3 overexpression is associated with HCC development in *Ncoa5*$^{+/-}$ *Tip30*$^{+/-}$ female mice.

HCN3 expression is regulated by the female hormone progesterone and progesterone receptors

Since multiple progesterone (Pg) response elements (PREs) were predicated in the putative promoter region of *HCN3* using PROMO (Figure 4A),[41,42] we tested whether Pg receptors (PRs) and Pg transcriptionally regulated HCN3. Human PLC/PRF/5 HCC cells with endogenous expression of NCOA5 and TIP30 (Figure S4A) were cotransfected with human progesterone receptor A (PRA) or B (PRB) expression vectors and a luciferase reporter plasmid containing a promoter region with nine PREs of the *HCN3* gene (Figure 4A). Cotransfection of PRB-expressing vectors, but not PRA-expressing vectors, increased luciferase activities in cells without Pg. Treating cells with Pg produced a 2.6- or 3.6-fold increase in luciferase activity in cells transfected with PRA or PRB, respectively (Figure 4B). Consistently, treatment of HCC cells transfected with PRA or PRB expression vector with Pg increased the mRNA levels of HCN3. PRB expression increased HCN3 mRNA levels in the absence of Pg (Figure 4C). Of note, HCC cells transfected with an empty vector also had increased HCN3 mRNA in response to Pg, which might be due to the activation of endogenous PRs by Pg. Low levels of endogenous PRB protein in PLC/PRF/5 cells were detected (Figure S4A), especially in the presence of proteasome inhibitor.[43] Cotransfection of the TIP30 expression vector reduced the luciferase activities in HCC cells with or without transfected PRA/PRB expression or Pg treatment (Figures 4D, 4E, and S4B). These results suggest that HCN3 expression is activated by the female hormone Pg and its receptors and repressed by TIP30.

HCN3 promotes HCC cell proliferation and protects HCC cells from ER stress

Ion channels have been known to play essential roles in cell-cycle progression,[44–46] and HCN3 was reported to promote breast cancer progression.[38] To test whether overexpressed HCN3 has oncogenic activity in the liver, we first confirmed the endogenous HCN3 expression in two different sex HCC cell lines, PLC/PRF/5 derived from a male patient and SNU-387 derived from a female patient that also express NCOA5 and TIP30 (Figure S4A), as well as in the mouse immortal NIH/3T3 fibroblast cells (Figure 5A). The cell growth was examined in media containing either high or low concentrations of serum to minimize influences from nutrients, growth factors, and inhibitors in the serum. Ectopic expression of HCN3 promoted the growth of all three cell lines in the low-serum conditions and NIH/3T3 and PLC/PRF/5 cells in the higher-serum conditions (Figure 5B). It also increased the soft agar colony-formation ability of PLC/PRF/5 cells (Figure 5C). Consistently, the CRISPR knockout of the *HCN3* gene in PLC/PRF/5 and SNU-387 cells significantly

decreased the growth of both cell lines compared to vector control cells (Figure 5D). The re-expression of HCN3 in the knockout cells complemented the cell-growth inhibition (Figure 5E). Moreover, the selective inhibitor for HCN channels, ZD7288,[37] inhibited the cell proliferation of both PLC/PRF/5 and SNU-387 cells in a dosage-dependent manner. However, the female-derived SNU-387 cells were more sensitive than the male-derived PLC/PRF/5 cells to ZD7288 treatment (Figure 5F). HCN3 overexpression also further increased the sensitivity of SNU-387 cells to HCN inhibition (Figure 5F). HCN3 was previously reported to affect the cell cycle and apoptosis by inhibiting ER stress in breast cancer cells.[38] To assess the similar impact of HCN3 on HCC cells, we treated the HCC cells with the ER-stress inducer thapsigargin in combination with ZD7288. In ER-stressed conditions, the sensitivity to ZD7288 was significantly increased in both cell lines (Figure S4C). HCN3 knockout in PLC/PRF/5 cells also sensitized the cell to ER-stress-induced cell-growth suppression (Figure S4D). Together, these results indicated that HCN3 promotes cell proliferation and protects against ER stress in HCC cells with a female preference *in vitro*.

HCN3 cooperates with MYC to promote the initiation and progression of HCC, and *Hcn3* knockout preferentially hinders MYC/MCL1-induced HCC development in female mice

To examine the oncogenic role of HCN3 overexpression *in vivo*, we used the Sleeping Beauty transposon system and the hydrodynamic tail vein injection technique to achieve stable overexpression of genes, specifically in the hepatocyte of mice.[47] As *MYC* overexpression alone was shown to be insufficient to induce liver cancer in BALB/c genetic background,[48] we chose to overexpress human *MYC* and *HCN3* simultaneously to induce oncogenesis. Injection of *MYC*- and *HCN3*-expressing vectors increased the incidence and volume of liver tumors compared to injection of the MYC-expressing vector and the empty vector in female BALB/c mice (although not statistically significantly) (Figures 6A and 6B). Histology analysis revealed that all liver tumors were moderately or poorly differentiated HCC. Remarkably, at least 50% of the tumors from female mice injected with *MYC*- and *HCN3*-expressing vectors were collision-type tumors consisting of moderately or poorly differentiated HCC and small round undifferentiated cancer cells (Figure 6C). Two out of eight HCC-bearing mice injected with *MYC*- and *HCN3*-expressing vectors had metastatic diseases, one of which had those small round undifferentiated cells metastasized to the ovaries of both sides, while the other had metastasis in the pancreas (Figures 6C and S4E). In contrast, liver tumors with *MYC* overexpression alone were all moderately differentiated HCC (Figure 6C), and no collision tumor or metastasis was detected in those mice. In mice injected with *MYC*- and *HCN3*-expressing vectors, HCC and small round undifferentiated cells in the liver collision tumors and small round undifferentiated cells in the ovary expressed ectopic HCN3, albumin, and AFP, indicating that the cell origins of these collision tumors are possibly the hepatocyte or liver progenitor (Figures 6C and S4F). These tumors also expressed more proliferation marker Ki-67 than liver HCCs from mice injected with *MYC*-expressing vector only (Figures 6C and S4F).

Hydrodynamic injection of *MYC*- and *MCL1*-expressing vectors were reported to induce 100% penetrant multiple liver tumors in female FVB/N mice[26] and mice with different genetic backgrounds, including the BALB/c strain.[48] Consistently, we observed liver tumors

with 100% penetrance and similar tumor volumes between male and female wild-type BALB/c mice injected with *MYC*- and *MCL1*-expressing vectors (Figure S4G). Hepatic *MYC* and *MCL1* overexpression in the same way resulted in 75% or 100% liver tumor penetrance in female or male BALB/c *Hcn3*$^{-/-}$ mice,[49] respectively. Importantly, liver tumor number and size were dramatically lower in *Hcn3*$^{-/-}$ female mice than in *Hcn3*$^{-/-}$ male mice (Figure 6D). Collectively, these results suggest that HCN3 is a cancer driver that can cooperate with MYC to promote the initiation and progression of poorly differentiated HCC, and the lack of HCN3 preferentially hinders hepatic tumorigenesis in female mice.

HCN3 is amplified and overexpressed in human HCC and correlated with poor survival, especially in female patients

To determine the clinical relevance of our findings on the upregulated cation transport pathways and HCN3 overexpression in the mice, we first used single-sample gene set enrichment analysis (ssGSEA) to compare the enrichment of GO.bp pathways in HCC samples from male and female patients in the TCGA cohort.[50] Strikingly, 33 GO.bp pathways related to cation transport are significantly more enriched in HCC specimens from female patients than from male patients (Figure S5). Next, we examined the protein expression of HCN3 in primary HCC samples from male and female patients using IHC staining on a tissue microarray. HCN3 expression was significantly higher in female HCCs than in male HCCs (Figure 7A). In the TCGA liver hepatocellular carcinoma (LIHC) cohort, HCN3 mRNA expression was significantly upregulated in HCCs compared to adjacent non-cancerous liver tissues (Figure 7B). Its mRNA levels appeared to be higher in female HCC adjacent liver tissues compared to male tissues (Figure S6A). Up to 24% of HCC samples (28% or 22% of female or male samples, respectively) had HCN3 alterations that were HCN3 gene amplification and mRNA overexpression (Figure 7C). Interestingly, HCC samples with HCN3 alterations had significantly lower TIP30 mRNA levels compared to samples without HCN3 alterations (Figure 7D). These alterations were mutually exclusive to *CTNNB1* mutation, amplification, or high expression in HCC (Figure 7C and Table S1). In those HCC samples with *HCN3* alterations, female HCC samples appeared to have higher HCN3 mRNA levels than those from males (Figure S6B). We then compared the transcriptome between HCCs with and without HCN3 alterations by assessing the enrichment of hallmark pathways using GSEA.[51] Pathways of the G_2M checkpoint, E2F targets, and mitotic spindle were highly enriched in HCC samples with HCN3 alterations, suggesting an increased cell proliferation in HCCs with HCN3 alterations, consistent with our *in vitro* and *in vivo* results (Figure 7E). When comparing the enrichment of hallmark pathways in HCC samples with and without HCN3 alterations using ssGSEA, we observed decreased inflammatory, reactive oxygen species, and androgen response pathways in HCC specimens with HCN3 alterations, besides the same upregulated pathways as suggested by GSEA (Figure 7F). Patients with these alterations had significantly worse survival and higher AFP level at procurement (Figures 7G, 7H, and S6C). Notably, female patients with HCN3 alterations had significantly poorer overall survival and disease-free survival than those without HCN3 alterations. At the same time, such differences were insignificant in male patients (Figures 7G and 7H; Table S2). Although the HCN3 alteration was associated with poorer HCC-specific survival and progression-free survival in both sexes, the associations were more significant and had a higher predicted hazard ratio in female

patients (Figures S6D and S6E). Together, these results suggest that HCN3 amplification and overexpression predict a poorer prognosis for HCC patients with a female preference and that HCN3 is a potential therapeutic target for personalized anti-HCC therapy.

DISCUSSION

In this study, we show for the first time that heterozygous deletion of *Tip30*, in the context of *Ncoa5* heterozygous deletion, preferentially promotes mouse HCC development in a female-biased manner. Unexpectedly, *Tip30* deletion did not cause a further increase of pro-inflammatory and p53 pathways in the preneoplastic liver of *Ncoa5*$^{+/-}$ female mice, unlike what was observed in the preneoplastic liver of *Ncoa5*$^{+/-}$ male mice, suggesting that TIP30 does not inhibit pro-inflammatory and p53-p21 pathways. Instead, we found significant overexpression of HCN3 in the livers of dual-mutant female mice compared to single-mutant female mice. In agreement with the observations in mice, HCN3 amplification and overexpression in human HCC specimens, ~28% of which had a history of chronic HBV infection, were more frequent in female patients than in male patients and were correlated with a poorer prognosis in female patients. HCN3 amplification and overexpression appeared mutually exclusive with the *CTNNB1* mutation. Several interpretations could explain this mutually exclusive event, one of which is that HCN3 overexpression possibly leads to the same outcome as *CTNNB1* mutations. *CTNNB1* mutations are known to occur preferentially in male HCC patients,[53] especially those infected with HBV.[54] We propose that female HCC patients might preferentially overexpress HCN3 in hepatocytes to drive liver oncogenesis, given the higher HCN3 levels in female HCCs and HCC adjacent liver tissues (Figures 7A, S6A, and S6B). In support of this possibility, we show that HCN3 expression could be enhanced by the female sex hormone Pg and its receptors. Moreover, HCN3 increases HCC cell proliferation *in vitro* and cooperates with MYC to promote the initiation and progression of HCC in female mice *in vivo*. Genetic knockout of *Hcn3* preferentially hinders HCC development in female mice induced by MYC and MCL1. Collectively, our data establish TIP30 and NCOA5 as crucial tumor suppressors in suppressing hepatocarcinogenesis in females and suggest that HCN3 is a female-biased cancer driver for liver oncogenesis. However, it remains to be determined how TIP30 and NCOA5 regulate HCN3 expression controlled by Pg-activated PRs as well as estrogen and androgen signaling pathways.

Cancer cells are known to overexpress ion channels to drive malignant behavior. Notably, HCN ion channel family members, including HCN3, serving as non-selective voltage-gated cation channels in the plasma membranes of cells, have been implicated in controlling cell-cycle progression. Consistently, HCN3 blockage inhibits the proliferation and cell-cycle progression of stem cells.[46,55] HCN3 has been reported to be overexpressed in breast, renal, and colorectal cancers and to be associated with poor survival outcomes in breast and renal cancer patients.[56] HCN3 inhibition has been shown to suppress breast cancer cell proliferation and tumor growth in patient-derived breast cancer xenograft models, suggesting HCN3 as a new molecular target that could be developed into targeted therapy for breast cancer patients.[38] Mechanistically, HCN3 might regulate the cell cycle, ER stress, and apoptosis through various mechanisms including cell-volume regulation, membrane potential modulation, generation of driving for Ca^{2+}, and protein-protein

interaction.[38,44,45,57] Our findings are in line with previous studies and suggest that HCN3 overexpression in HCC cells promotes cell proliferation via a similar mechanism, making it a potential therapeutic target for personalized anti-HCC therapy.

In addition to HCN3, other genes dysregulated by NCOA5 and TIP30 deficiency in the female mouse livers might also contribute to HCC development in *Ncoa5*$^{+/-}$ *Tip30*$^{+/-}$ female mice. One of these genes is *Mycn*, a member of the *myc* proto-oncogene family, which was overexpressed at the mRNA level in the livers of *Ncoa5*$^{+/-}$ *Tip30*$^{+/-}$ female mice. Analysis of the TCGA cohort of human HCC specimens revealed that *MYCN* amplification and gain occurred more frequently in female patients than in male patients, with an incidence of 26% in females compared to 12% in males (Figure S7A). Interestingly, *MYCN* amplification and overexpression co-occurred with *HCN3* amplification and overexpression in female patients but not male patients (Table S3). Moreover, the concurrence of *MYCN* alterations and *HCN3* overexpression was associated with decreased *TIP30* mRNA in female patients but not in males (Figures S7B and S7C). As *MYCN* is known to be an oncogene, its overexpression likely contributes significantly to female-biased HCC development. However, further experiments are necessary to determine the collaborative role of HCN3 and MYCN in promoting HCC development.

In conclusion, this study highlights that female hepatocarcinogenesis could be driven by a female-biased mechanism regulated by NCOA5 and TIP30. Our work also suggests the ion channel HCN3 as a female-biased HCC driver, providing a possible personalized therapeutic target for treating female patients with HCC.

Limitations of the study

To identify a female-biased mechanism underlying HCC development, we prioritized our investigation on identifying early transcriptomic alterations in the livers of *Ncoa5*$^{+/}$ *Tip30*$^{+/-}$ female mice by analyzing liver transcriptomes of 5-month-old *Ncoa5*$^{+/}$ *Tip30*$^{+/-}$ and control female mice. However, this approach is unable to discover genes altered in cells of other organs and tissues, such as different immune cells, which could systematically affect tumor surveillance in a female-biased manner, thereby contributing to HCC development in mice. Moreover, this approach does not identify critical cancer drivers altered in the later steps of hepatocarcinogenesis and the genomic mutations necessary for hepatocyte malignant transformation in *Ncoa5*$^{+/-}$ *Tip30*$^{+/-}$ female mice. Finally, our biochemical studies on transcriptional regulation of HCN3 by TIP30 and progesterone *in vitro* might not reflect sex-mediated regulation *in vivo*.

STAR★METHODS

RESOURCE AVAILABILITY

Lead contact—Further information and requests for resources and reagents should be directed to and will be fulfilled by the lead contact, Hua Xiao (xiaoh@msu.edu).

Materials availability—New plasmids and mouse lines generated in this study are available upon request. Requests for plasmids and mouse lines should be directed to and will be fulfilled by the lead contact with an institutional material transfer agreement.

Data and code availability

- Raw and processed RNA-sequencing data have been deposited at GEO and are publicly available as of the date of publication. Accession numbers are listed in the Key resources table. The rest of the data reported in this paper will be shared by the lead contact upon request.
- This paper does not report original code.
- Any additional information required to reanalyze the data reported in this paper is available from the lead contact upon request.

EXPERIMENTAL MODEL AND STUDY PARTICIPANT DETAILS

Mice—Generation of *Ncoa5* or *Tip30* deficient mice was described previously.[8,28,34] Double deficient BALB/c *Ncoa5*$^{+/-}$ *Tip30*$^{+/-}$ mice and control *Ncoa5*$^{+/-}$, *Tip30*$^{+/-}$, and wild-type mice were generated by crossing *Ncoa5*$^{+/-}$ female mice and *Tip30*$^{+/-}$ male mice because male *Ncoa5*$^{+/-}$ mice were infertile.[8,70] *Hcn3*$^{-/-}$ C57BL/6 mice provided by Dr. Martin Biel[49] were backcrossed for seven generations to the BALB/c genetic background. Wild-type BALB/c mice used in the hydrodynamic tail vein injection experiments were purchased from the Jackson Laboratory. BALB/c male and female mice were allocated to experimental groups randomly for hydrodynamic tail vein injection experiments or according to genotypes for spontaneous tumor development experiments. All mice were under a standard normal diet and 12 h light/12 h dark cycle at the Michigan State University animal facilities and housed in Optimice cages. All experimental procedures on mice were approved by the Michigan State University Institutional Animal Care and Use Committee and were performed in accordance with their regulatory standards.

Cell lines—Mouse fibroblast NIH/3T3 (derived from male), human kidney cell HEK293T (derived from female), and human liver cancer cell line PLC/PRF/5 (derived from male) and SNU-387 (derived from female) were purchased from ATCC. Cell lines were authenticated by STR profiling. SNU-387 cells were cultured using ATCC-formulated RPMI-1640 medium supplemented with 10% fetal bovine serum (FBS), 100 U/mL of penicillin, and 100 μg/mL of streptomycin at 37°C in 5% CO_2. Other cell lines were cultured using DMEM high glucose medium (Thermo Fisher) supplemented with 10% FBS, 100 U/mL of penicillin, and 100 μg/mL of streptomycin. For hormone treatment experiments, cells were cultured and treated in phenol red-free DMEM (Thermo Fisher) supplemented with charcoal-stripped FBS (Biowest). Proteasome inhibition was induced by treatment of 10 μM of (R)-MG132 (Cayman Chemical) for 6 h. Selective HCN blocker ZD7288 was purchased from Tocris. Thapsigargin was purchased from Millipore-Sigma. Cells were treated with ZD7288 in a complete medium for 3 days.

METHOD DETAILS

Transcriptomic analyses of human samples—Processed gene expression, copy number variation, mutation, and clinical data of the TCGA LIHC cohort were retrieved with UCSC Xena and cBioportal.[52,62–64] Differences in gene mRNA levels between TCGA patient subgroups were determined with the comparison functionality of cBioportal.[64] Protein-protein interaction network of gene products of interest was analyzed using

STRING.[65] For pathway analyses, Gene Set Enrichment Analysis (GSEA) version 4.2.1 and ssGSEA v10 were used[50,51] and carried out on GenePattern.

Quantitative PCR and mouse transcriptome analyses—Total RNA was isolated using TRIzol (Thermo Fisher) according to the manufacturer's instructions. RNA for high throughput sequencing was isolated using a combined TRIzol and RNeasy Mini Kit (Qiagen) method according to the manufacturer's instructions. cDNA was generated using SuperScript IV First-Strand Synthesis System (Thermo Fisher) according to the manufacturer's instructions. Quantitative real-time PCR was performed on a QuantStudio 3 Real-Time PCR machine using the PowerUp SYBR Green reagent (Thermo Fisher). PCR primer sequences are available in Table S4.

Isolated total RNA from mouse liver was first quality-controlled using Nanodrop Spectrophotometer (Thermo Fisher) and Bio-analyzer System (Agilent). Total RNA was then sent to Novogene, which carried out further RNA quality control, mRNA selection, cDNA library preparation, sequencing with a NovaSeq 6000 (Illumina), raw data quality control, and raw data delivery. Raw data were then trimmed to remove low-quality reads and adapter reads using Trimmomatic[66] and aligned to the Ensembl GRCm38 genome using STAR.[67] Count normalization and differential gene expression analysis were conducted using DESeq2.[68] Pathway analysis was performed using GAGE.[69]

Histological and serological analyses—Neutrally buffered 10% formalin solution (Sigma-Aldrich) fixed mouse tissues were sent to the Investigative Histopathology Laboratory of Michigan State University and processed, embedded, sectioned, and H & E stained. Liver histological features were scored using the Modified Hepatic Activity Index system.[36] Mouse blood was freshly collected, and serum was separated by centrifugation. Serum a-fetoprotein levels were quantified using the mouse AFP Quantikine ELISA kit (R&D Systems) according to the manufacturer's instructions. Serum ALT activity was quantified using the Alanine Transaminase Colorimetric Activity Assay Kit (Cayman Chemical) according to the manufacturer's instructions. Liver tissue IL-6 levels were quantified using the mouse IL-6 ELISA Kit (Proteintech). Absorbance was read by a FLUOstar OPTIMA microplate reader (BMG LABTECH).

Immunohistochemistry—Immunohistochemistry staining was performed using the VECTASTAIN ABC-HRP system (Vector Laboratories) according to the manufacturer's instructions. IHC staining intensity was scored using the IRS system.[39] The human HCC tissue array (LV1505a) was purchased from TissueArray.Com LLC, and the clinical information of patients included in the array is available on the supplier's website.

Lentiviral gene expression—The coding sequence of the human *HCN3* gene was amplified and HA-tagged from the plasmid HsCD00348243 (DF/HCC DNA Resource Core), which contains the consensus coding sequence of human *HCN3* (CCDS 1108.1). The sequence was then cloned into the pSin-EF2-Pur vector[58] (Addgene). Polyethyleneimine-mediated transfection of HCN3 or GFP expression plasmids with pCMV delta R8.2 packaging plasmid (Addgene) and pMD2.G envelope plasmid (Addgene) was performed on HEK293T cells, and lentivirus was collected after transfection. Cells stably overexpressing

HCN3 or control protein were established by infecting cells with lentivirus and selected by puromycin.

Soft agar colony formation assay—Soft agar colony formation assay was performed as described.[71] Briefly, 6-well plates were plated with a bottom layer of 0.5% agar in DMEM medium and a top layer of 0.3% agar in DMEM medium containing 5000 cells/well. Cells were cultured for 21 days while maintaining a layer of growth medium on top. Cells were finally stained with Nitrotetrazolium Blue chloride (Sigma-Aldrich), and photos were captured under a microscope. Colony number and size were analyzed using ImageJ.

CRISPR/Cas-mediated gene knockout—The CRISPR/Cas9 mediated HCN3 knockout was achieved using the pSpCas9(BB)-2A-Puro (PX459) V2.0 plasmid[59] obtained from Addgene, and the following guide sequences were used: target 1 (exon 6): CGGGACACACGCCTCACCGA; target 2 (exon 5): GAGCGAGCCGCTTCGCGAGG. The guide target sequences and PAMs were cloned into the PX459 vector according to a cloning protocol described on Addgene. Cells were transfected with vector control or targeting constructs using Lipofectamine 3000 (Thermo Fisher) according to the manufacturer's instructions and were then selected with 2 μg/mL puromycin. Selected cells were cultured in single clones, and genomic DNA was extracted using QuickExtract (Lucigen), and gene knockout was validated by PCR, sanger sequencing, and western blotting.

Cell proliferation assay—1 or 1.5×10^3 cells were seeded in 96-well plates and cultured for 2 to 4 days in DMEM medium containing 10%, 2%, or 0.2% FBS. For HCN3 inhibition and thapsigargin treatment experiments, 1 or 2.5×10^3 cells in DMEM medium containing 10% FBS were seeded in 96-well plates and treated for 72 h. CCK-8 (Dojindo) was used to determine the relative cell growth according to the manufacturer's instructions. Absorbance was read by a FLUOstar OPTIMA microplate reader (BMG LABTECH).

Western blotting—Protein was isolated from tissue and cell samples using RIPA buffer (Thermo Fisher) or Laemmli Sample Buffer (BIO-RAD). SDS-PAGE of processed protein samples was performed using BIORAD Mini-protein TGX gels. LICOR IRDye secondary antibodies were used for fluorescent detection, and photos were captured using the LICOR Odyssey Imaging system. Quantification was performed using LICOR Odyssey and Image Studio software.

Dual-luciferase reporter assay—Transcription factor binding site prediction was performed using PROMO.[41,42] The genomic DNA fraction from −742 to +752 bp relative to the HCN3 transcription start site containing the putative promoter region was amplified from MCF-7 genomic DNA. This fraction includes the SNP rs12749306, which has an ALFA allele frequency of 26.6%. The fraction was cloned into the pGL2-Basic vector (Promega) to get the pGL2-promoHCN3. Human TIP30 expression plasmid pcDNA3-TIP30 was previously described.[60] pcDNA3-hPRA and pcDNA3-hPRB expression plasmids were obtained from Addgene.[61] pRL (Promega) was used as the control reporter. Cells were transfected with pRL, pGL2-promoHCN3, and other expression plasmids using Lipofectamine 3000 (Thermo Fisher) according to the manufacturer's instructions. The treatment of cells started 24 h after transfection, and cells were processed 48h

after transfection and tested for luciferase activity using the Dual-Luciferase Reporter Assay System (Promega). The bioluminescence signal was read by a Veritas Microplate Luminometer (Turner Biosystems).

Hydrodynamic tail vein injection for stable gene expression in hepatocytes— pT3-EF1α-*c*-MYC, pT3-EF1α-MCL1, and pCMV/SB plasmids were kindly provided by Dr. Xin Chen.[48] The pT3-EF1α-*c*-MYC plasmid was manipulated to generate pT3-EF1α-HCN3 carrying the HA-tagged human HCN3 coding sequence and pT3-EF1α empty vector (EV). Different combinations of plasmids were injected into 7-week-old wild-type or *Hcn3*$^{-/-}$ male and female BALB/c mice according to the published method.[48] A total of 20 μg of pT3-EF1α-*c*-MYC, 20 μg of EV, and 1.6 μg of pCMV/SB (wild-type female BALB/c mice), or a total of 20 μg of pT3-EF1α-*c*-MYC, 20 μg of pT3-EF1α-HCN3, and 1.6 μg of pCMV/SB (wild-type female BALB/c mice), or a total of 10 μg of pT3-EF1α-*c*-MYC, 5 μg of pT3-EF1α-MCL1, and 0.6 μg of pCMV/SB (wild-type and *Hcn3*$^{-/-}$ male and female BALB/c) in 2 mL of 0.9% NaCl solution were injected to each mouse. Mice that received *MCL1* overexpression were monitored for liver tumor formation for 8 weeks, and mice that received other injections were monitored for 14 weeks or until morbid and then euthanized and necropsied.

Antibodies—Primary antibodies used in this study include anti: Mac-2 (Galectin-3, CL8942AP) by Cedarlane Labs; IL-6 (sc-1265), Na^+/K^+-ATPases (sc-48345), and β-Actin (sc-47778) by Santa Cruz Biotechnology; HCN3 (ab84818) by Abcam; HCN3 (APC-057) by Alomone Labs; HCN3 (MA3–902) by Thermo Fisher; HA-tag (#3724) and PR (#8757) by Cell Signaling Technology; AFP (14550–1-AP) and Albumin (16475–1-AP) by Proteintech; Ki-67 (AB9260) by Millipore-Sigma; NCOA5 (A300–790A) by Bethyl; TIP30 made by Xiao Lab which was described previously.[28]

QUANTIFICATION AND STATISTICAL ANALYSIS

All data are shown as mean ± SEM if not specified otherwise. Statistical significance of differences was determined by one-way ANOVA Tukey's multiple comparison test, two-way ANOVA Tukey's multiple comparison test and Sidak's multiple comparison test, two-tailed unpaired Student's t-test, Welch's t test with the FDR methods, Pearson's correlation two-tailed significance test, Chi-squared test, Mann-Whitney U test, or log rank test in GraphPad Prism 7 with details listed in the corresponding figure legends. ****$p < 0.0001$, ***$p < 0.001$, **$p < 0.01$, *$p < 0.05$, ns = not significant.

Supplementary Material

Refer to Web version on PubMed Central for supplementary material.

ACKNOWLEDGMENTS

This work was supported by a National Cancer Institute grant (R01 CA188305), the Discretionary Funding Initiative grants of Michigan State University (GR101538 and GR100453) to H.X., and a cancer research grant to H.X. and Q.-S.M provided by the Henry Ford Health and Michigan State University Health Sciences. Y.Z. was partially supported by the Aitch Fellowship of the Aitch Foundation and dissertation continuation and completion fellowships of the Graduate School of Michigan State University. X.L., Y.L., and A.L. were supported by fellowships from the Integrated Hospital of Traditional Chinese Medicine, Southern Medical University.

The authors thank Xin Chen for the gifts of pt3 and SB vectors and members of the H.X. lab for helpful discussions. The results reported here are partially based on data generated by the TCGA Research Network (http://cancergenome.nih.gov), which we also gratefully acknowledge.

REFERENCES

1. Llovet JM, Zucman-Rossi J, Pikarsky E, Sangro B, Schwartz M, Sherman M, and Gores G. (2016). Hepatocellular carcinoma. Nat. Rev. Dis. Primers 2, 16018. 10.1038/nrdp.2016.18.
2. Jemal A, Ward EM, Johnson CJ, Cronin KA, Ma J, Ryerson B, Mariotto A, Lake AJ, Wilson R, Sherman RL, et al. (2017). Annual Report to the Nation on the Status of Cancer, 1975–2014, Featuring Survival. J. Natl. Cancer Inst. 109, djx030. 10.1093/jnci/djx030.
3. Siegel RL, Miller KD, and Jemal A. (2019). Cancer statistics, 2019. CA. Cancer J. Clin. 69, 7–34. 10.3322/caac.21551. [PubMed: 30620402]
4. El-Serag HB, and Rudolph KL (2007). Hepatocellular carcinoma: epidemiology and molecular carcinogenesis. Gastroenterology 132, 2557–2576. 10.1053/j.gastro.2007.04.061. [PubMed: 17570226]
5. Nakatani T, Roy G, Fujimoto N, Asahara T, and Ito A. (2001). Sex hormone dependency of diethylnitrosamine-induced liver tumors in mice and chemoprevention by leuprorelin. Jpn. J. Cancer Res. 92, 249–256. 10.1111/j.1349-7006.2001.tb01089.x. [PubMed: 11267934]
6. Ma WL, Hsu CL, Wu MH, Wu CT, Wu CC, Lai JJ, Jou YS, Chen CW, Yeh S, and Chang C. (2008). Androgen receptor is a new potential therapeutic target for the treatment of hepatocellular carcinoma. Gastroenterology 135, 947–955–955.e1–5. 10.1053/j.gastro.2008.05.046.
7. Kemp CJ, and Drinkwater NR (1989). Genetic variation in liver tumor susceptibility, plasma testosterone levels, and androgen receptor binding in six inbred strains of mice. Cancer Res. 49, 5044–5047. [PubMed: 2766275]
8. Gao S, Li A, Liu F, Chen F, Williams M, Zhang C, Kelley Z, Wu CL, Luo R, and Xiao H. (2013). NCOA5 haploinsufficiency results in glucose intolerance and subsequent hepatocellular carcinoma. Cancer Cell 24, 725–737. 10.1016/j.ccr.2013.11.005. [PubMed: 24332041]
9. Haupt S, Caramia F, Klein SL, Rubin JB, and Haupt Y. (2021). Sex disparities matter in cancer development and therapy. Nat. Rev. Cancer 21, 393–407. 10.1038/s41568-021-00348-y. [PubMed: 33879867]
10. Sykiotis GP, Pitteloud N, Seminara SB, Kaiser UB, and Crowley WF Jr. (2010). Deciphering genetic disease in the genomic era: the model of GnRH deficiency. Sci. Transl. Med. 2, 32rv2. 10.1126/scitranslmed.3000288.
11. Wang SH, Yeh SH, Lin WH, Yeh KH, Yuan Q, Xia NS, Chen DS, and Chen PJ (2012). Estrogen receptor alpha represses transcription of HBV genes via interaction with hepatocyte nuclear factor 4alpha. Gastroenterology 142, 989–998.e4. 10.1053/j.gastro.2011.12.045. [PubMed: 22240483]
12. Nault JC, Martin Y, Caruso S, Hirsch TZ, Bayard Q, Calderaro J, Charpy C, Copie-Bergman C, Ziol M, Bioulac-Sage P, et al. (2020). Clinical Impact of Genomic Diversity From Early to Advanced Hepatocellular Carcinoma. Hepatology 71, 164–182. 10.1002/hep.30811. [PubMed: 31206197]
13. Jackson SS, Marks MA, Katki HA, Cook MB, Hyun N, Freedman ND, Kahle LL, Castle PE, Graubard BI, and Chaturvedi AK (2022). Sex disparities in the incidence of 21 cancer types: Quantification of the contribution of risk factors. Cancer 128, 3531–3540. 10.1002/cncr.34390. [PubMed: 35934938]
14. Li CH, Haider S, Shiah YJ, Thai K, and Boutros PC (2018). Sex Differences in Cancer Driver Genes and Biomarkers. Cancer Res. 78, 5527–5537. 10.1158/0008-5472.CAN-18-0362. [PubMed: 30275052]
15. Yuan Y, Liu L, Chen H, Wang Y, Xu Y, Mao H, Li J, Mills GB, Shu Y, Li L, and Liang H. (2016). Comprehensive Characterization of Molecular Differences in Cancer between Male and Female Patients. Cancer Cell 29, 711–722. 10.1016/j.ccell.2016.04.001. [PubMed: 27165743]
16. Natri HM, Wilson MA, and Buetow KH (2019). Distinct molecular etiologies of male and female hepatocellular carcinoma. BMC Cancer 19, 951. 10.1186/s12885-019-6167-2. [PubMed: 31615477]

17. Ye W, Siwko S, and Tsai RYL (2021). Sex and Race-Related DNA Methylation Changes in Hepatocellular Carcinoma. Int. J. Mol. Sci. 22, 3820. 10.3390/ijms22083820. [PubMed: 33917049]

18. Naugler WE, Sakurai T, Kim S, Maeda S, Kim K, Elsharkawy AM, and Karin M. (2007). Gender disparity in liver cancer due to sex differences in MyD88-dependent IL-6 production. Science 317, 121–124. 10.1126/science.1140485. [PubMed: 17615358]

19. Li Y, Xu A, Jia S, and Huang J. (2019). Recent advances in the molecular mechanism of sex disparity in hepatocellular carcinoma. Oncol. Lett. 17, 4222–4228. 10.3892/ol.2019.10127. [PubMed: 30988804]

20. Chen CL, Kuo MJ, Yen AMF, Yang WS, Kao JH, Chen PJ, and Chen HH (2020). Gender Difference in the Association Between Metabolic Factors and Hepatocellular Carcinoma. JNCI Cancer Spectr. 4, pkaa036. 10.1093/jncics/pkaa036.

21. Li Z, Tuteja G, Schug J, and Kaestner KH (2012). Foxa1 and Foxa2 are essential for sexual dimorphism in liver cancer. Cell 148, 72–83. 10.1016/j.cell.2011.11.026. [PubMed: 22265403]

22. Hartwell HJ, Petrosky KY, Fox JG, Horseman ND, and Rogers AB (2014). Prolactin prevents hepatocellular carcinoma by restricting innate immune activation of c-Myc in mice. Proc. Natl. Acad. Sci. USA. 111, 11455–11460. 10.1073/pnas.1404267111. [PubMed: 25049387]

23. Manieri E, Herrera-Melle L, Mora A, Tomás-Loba A, Leiva-Vega L, Fernández DI, Rodríguez E, Morá n L, Hernández-Cosido L, Torres JL, et al. (2019). Adiponectin accounts for gender differences in hepatocellular carcinoma incidence. J. Exp. Med. 216, 1108–1119. 10.1084/jem.20181288. [PubMed: 30944152]

24. Ji J, Shi J, Budhu A, Yu Z, Forgues M, Roessler S, Ambs S, Chen Y, Meltzer PS, Croce CM, et al. (2009). MicroRNA expression, survival, and response to interferon in liver cancer. N. Engl. J. Med. 361, 1437–1447. 10.1056/NEJMoa0901282. [PubMed: 19812400]

25. Kota J, Chivukula RR, O'Donnell KA, Wentzel EA, Montgomery CL, Hwang HW, Chang TC, Vivekanandan P, Torbenson M, Clark KR, et al. (2009). Therapeutic microRNA delivery suppresses tumorigenesis in a murine liver cancer model. Cell 137, 1005–1017. 10.1016/j.cell.2009.04.021. [PubMed: 19524505]

26. Ji F, Zhang J, Liu N, Gu Y, Zhang Y, Huang P, Zhang N, Lin S, Pan R, Meng Z, et al. (2022). Blocking hepatocarcinogenesis by a cytochrome P450 family member with female-preferential expression. Gut 71, 2313–2324. 10.1136/gutjnl-2021-326050. [PubMed: 34996827]

27. Xu C, Cheng S, Chen K, Song Q, Liu C, Fan C, Zhang R, Zhu Q, Wu Z, Wang Y, et al. (2023). Sex Differences in Genomic Features of Hepatitis B-Associated Hepatocellular Carcinoma With Distinct Antitumor Immunity. Cell. Mol. Gastroenterol. Hepatol. 15, 327–354. 10.1016/j.jcmgh.2022.10.009. [PubMed: 36272708]

28. Ito M, Jiang C, Krumm K, Zhang X, Pecha J, Zhao J, Guo Y, Roeder RG, and Xiao H. (2003). TIP30 deficiency increases susceptibility to tumorigenesis. Cancer Res. 63, 8763–8767. [PubMed: 14695192]

29. Yu X, Li Z, and Wu WKK (2014). TIP30: A Novel Tumor-Suppressor Gene. Oncol. Res. 22, 339–348. 10.3727/096504015X14424348426116. [PubMed: 26629947]

30. Jiang C, Ito M, Piening V, Bruck K, Roeder RG, and Xiao H. (2004). TIP30 interacts with an estrogen receptor alpha-interacting coactivator CIA and regulates c-myc transcription. J. Biol. Chem. 279, 27781–27789. 10.1074/jbc.M401809200. [PubMed: 15073177]

31. Williams M, Liu X, Zhang Y, Reske J, Bahal D, Gohl TG, Hollern D, Ensink E, Kiupel M, Luo R, et al. (2020). NCOA5 deficiency promotes a unique liver protumorigenic microenvironment through p21(WAF1/CIP1) overexpression, which is reversed by metformin. Oncogene 39, 3821–3836. 10.1038/s41388-020-1256-x. [PubMed: 32203160]

32. Dhar D, Seki E, and Karin M. (2014). NCOA5, IL-6, type 2 diabetes, and HCC: The deadly quartet. Cell Metab. 19, 6–7. 10.1016/j.cmet.2013.12.010. [PubMed: 24411937]

33. Facciorusso A, and Barone M. (2014). Glucose intolerance and hepatocellular carcinoma: recent findings for old diseases. Hepatobiliary Surg. Nutr. 3, 91–92. 10.3978/j.issn.2304-3881.2014.02.15. [PubMed: 24812601]

34. Li A, Zhang C, Gao S, Chen F, Yang C, Luo R, and Xiao H. (2013). TIP30 loss enhances cytoplasmic and nuclear EGFR signaling and promotes lung adenocarcinogenesis in mice. Oncogene 32, 2273–2281–2281e.1–12. 10.1038/onc.2012.253.
35. Bosman FT, Carneiro F, Hruban RH, and Theise ND (2010). WHO Classification of Tumours of the Digestive System (World Health Organization).
36. Ishak K, Baptista A, Bianchi L, Callea F, De Groote J, Gudat F, Denk H, Desmet V, Korb G, MacSween RN, et al. (1995). Histological grading and staging of chronic hepatitis. J. Hepatol. 22, 696–699. 10.1016/0168-8278(95)80226-6. [PubMed: 7560864]
37. Stieber J, Stö ckl G, Herrmann S, Hassfurth B, and Hofmann F. (2005). Functional expression of the human HCN3 channel. J. Biol.Chem. 280, 34635–34643. 10.1074/jbc.M502508200. [PubMed: 16043489]
38. Mok KC, Tsoi H, Man EP, Leung MH, Chau KM, Wong LS, Chan WL, Chan SY, Luk MY, Chan JYW, et al. (2021). Repurposing hyperpolarization-activated cyclic nucleotide-gated channels as a novel therapy for breast cancer. Clin. Transl. Med. 11, e578. 10.1002/ctm2.578. [PubMed: 34841695]
39. Remmele W, and Stegner HE (1987). [Recommendation for uniform definition of an immunoreactive score (IRS) for immunohistochemical estrogen receptor detection (ER-ICA) in breast cancer tissue]. Pathologe 8, 138–140. [PubMed: 3303008]
40. Fedchenko N, and Reifenrath J. (2014). Different approaches for interpretation and reporting of immunohistochemistry analysis results in the bone tissue - a review. Diagn. Pathol. 9, 221. 10.1186/s13000-014-0221-9. [PubMed: 25432701]
41. Messeguer X, Escudero R, Farré D, Núñez O, Martínez J, and Albà MM (2002). PROMO: detection of known transcription regulatory elements using species-tailored searches. Bioinformatics 18, 333–334. 10.1093/bioinformatics/18.2.333. [PubMed: 11847087]
42. Farré D, Roset R, Huerta M, Adsuara JE, Roselló L, Albà MM, and Messeguer X. (2003). Identification of patterns in biological sequences at the ALGGEN server: PROMO and MALGEN. Nucleic Acids Res. 31, 3651–3653. 10.1093/nar/gkg605. [PubMed: 12824386]
43. Zhang C, Mori M, Gao S, Li A, Hoshino I, Aupperlee MD, Haslam SZ, and Xiao H. (2010). Tip30 deletion in MMTV-Neu mice leads to enhanced EGFR signaling and development of estrogen receptor-positive and progesterone receptor-negative mammary tumors. Cancer Res. 70, 10224–10233. 10.1158/0008-5472.CAN-10-3057. [PubMed: 21159643]
44. Urrego D, Tomczak AP, Zahed F, Stu€hmer W, and Pardo LA (2014). Potassium channels in cell cycle and cell proliferation. Philos. Trans. R. Soc. Lond. B Biol. Sci. 369, 20130094. 10.1098/rstb.2013.0094.
45. Koch KS, and Leffert HL (1979). Increased sodium ion influx is necessary to initiate rat hepatocyte proliferation. Cell 18, 153–163. 10.1016/0092-8674(79)90364-7. [PubMed: 509519]
46. Lau YT, Wong CK, Luo J, Leung LH, Tsang PF, Bian ZX, and Tsang SY (2011). Effects of hyperpolarization-activated cyclic nucleotide-gated (HCN) channel blockers on the proliferation and cell cycle progression of embryonic stem cells. Pflugers Arch. 461, 191–202. 10.1007/s00424-010-0899-9. [PubMed: 21110038]
47. Chen X, and Calvisi DF (2014). Hydrodynamic transfection for generation of novel mouse models for liver cancer research. Am. J. Pathol. 184, 912–923. 10.1016/j.ajpath.2013.12.002. [PubMed: 24480331]
48. Méndez-Lucas A, Li X, Hu J, Che L, Song X, Jia J, Wang J, Xie C, Driscoll PC, Tschaharganeh DF, et al. (2017). Glucose Catabolism in Liver Tumors Induced by c-MYC Can Be Sustained by Various PKM1/PKM2 Ratios and Pyruvate Kinase Activities. Cancer Res. 77, 4355–4364. 10.1158/0008-5472.CAN-17-0498. [PubMed: 28630053]
49. Fenske S, Mader R, Scharr A, Paparizos C, Cao-Ehlker X, Michalakis S, Shaltiel L, Weidinger M, Stieber J, Feil S, et al. (2011). HCN3 contributes to the ventricular action potential waveform in the murine heart. Circ. Res. 109, 1015–1023. 10.1161/CIRCRE-SAHA.111.246173. [PubMed: 21903939]
50. Barbie DA, Tamayo P, Boehm JS, Kim SY, Moody SE, Dunn IF, Schinzel AC, Sandy P, Meylan E, Scholl C, et al. (2009). Systematic RNA interference reveals that oncogenic KRAS-driven cancers require TBK1. Nature 462, 108–112. 10.1038/nature08460. [PubMed: 19847166]

51. Subramanian A, Tamayo P, Mootha VK, Mukherjee S, Ebert BL, Gillette MA, Paulovich A, Pomeroy SL, Golub TR, Lander ES, and Mesirov JP (2005). Gene set enrichment analysis: a knowledge-based approach for interpreting genome-wide expression profiles. Proc. Natl. Acad. Sci. USA. 102, 15545–15550. 10.1073/pnas.0506580102. [PubMed: 16199517]
52. Liu J, Lichtenberg T, Hoadley KA, Poisson LM, Lazar AJ, Cherniack AD, Kovatich AJ, Benz CC, Levine DA, Lee AV, et al. (2018). An Integrated TCGA Pan-Cancer Clinical Data Resource to Drive High-Quality Survival Outcome Analytics. Cell 173, 400–416.e11. 10.1016/j.cell.2018.02.052. [PubMed: 29625055]
53. Dow M, Pyke RM, Tsui BY, Alexandrov LB, Nakagawa H, Taniguchi K, Seki E, Harismendy O, Shalapour S, Karin M, et al. (2018). Integrative genomic analysis of mouse and human hepatocellular carcinoma. Proc. Natl. Acad. Sci. USA. 115, E9879–E9888. 10.1073/pnas.1811029115. [PubMed: 30287485]
54. Martínez-Jiménez F, Muiños F, Sentís I, Deu-Pons J, Reyes-Salazar I, Arnedo-Pac C, Mularoni L, Pich O, Bonet J, Kranas H, et al. (2020). A compendium of mutational cancer driver genes. Nat. Rev. Cancer 20, 555–572. 10.1038/s41568-020-0290-x. [PubMed: 32778778]
55. Omelyanenko A, Sekyrova P, and Andäng M. (2016). ZD7288, a blocker of the HCN channel family, increases doubling time of mouse embryonic stem cells and modulates differentiation outcomes in a context-dependent manner. SpringerPlus 5, 41. 10.1186/s40064-016-1678-7. [PubMed: 26835223]
56. Phan NN, Huynh TT, and Lin YC (2017). Hyperpolarization-activatedcyclic nucleotide-gated gene signatures and poor clinical outcome of cancer patient. Transl. Cancer Res. 6, 698–708. 10.21037/tcr.2017.07.22.
57. Johard H, Omelyanenko A, Fei G, Zilberter M, Dave Z, Abu-Youssef R, Schmidt L, Harisankar A, Vincent CT, Walfridsson J, et al. (2020). HCN Channel Activity Balances Quiescence and Proliferation in Neural Stem Cells and Is a Selective Target for Neuroprotection During Cancer Treatment. Mol. Cancer Res. 18, 1522–1533. 10.1158/1541-7786.MCR-20-0292. [PubMed: 32665429]
58. Yu J, Vodyanik MA, Smuga-Otto K, Antosiewicz-Bourget J, Frane JL, Tian S, Nie J, Jonsdottir GA, Ruotti V, Stewart R, et al. (2007). Induced pluripotent stem cell lines derived from human somatic cells. Science 318, 1917–1920. 10.1126/science.1151526. [PubMed: 18029452]
59. Ran FA, Hsu PD, Wright J, Agarwala V, Scott DA, and Zhang F(2013). Genome engineering using the CRISPR-Cas9 system. Nat. Protoc. 8, 2281–2308. 10.1038/nprot.2013.143. [PubMed: 24157548]
60. Zhang C, Li A, Zhang X, and Xiao H. (2011). A novel TIP30 protein complex regulates EGF receptor signaling and endocytic degradation. J. Biol. Chem. 286, 9373–9381. 10.1074/jbc.M110.207720. [PubMed: 21252234]
61. Su S, Blackwelder AJ, Grossman G, Minges JT, Yuan L, Young SL, and Wilson EM (2012). Primate-specific melanoma antigen-A11 regulates isoform-specific human progesterone receptor-B transactivation. J. Biol. Chem. 287, 34809–34824. 10.1074/jbc.M112.372797. [PubMed: 22891251]
62. Goldman MJ, Craft B, Hastie M, Repečka K, McDade F, Kamath A, Banerjee A, Luo Y, Rogers D, Brooks AN, et al. (2020). Visualizing and interpreting cancer genomics data via the Xena platform. Nat. Biotechnol. 38, 675–678. 10.1038/s41587-020-0546-8. [PubMed: 32444850]
63. Cerami E, Gao J, Dogrusoz U, Gross BE, Sumer SO, Aksoy BA,Jacobsen A, Byrne CJ, Heuer ML, Larsson E, et al. (2012). The cBio cancer genomics portal: an open platform for exploring multidimensional cancer genomics data. Cancer Discov. 2, 401–404. 10.1158/2159-8290.CD-12-0095. [PubMed: 22588877]
64. Gao J, Aksoy BA, Dogrusoz U, Dresdner G, Gross B, Sumer SO,Sun Y, Jacobsen A, Sinha R, Larsson E, et al. (2013). Integrative analysis of complex cancer genomics and clinical profiles using the cBioPortal. Sci. Signal. 6, pl1. 10.1126/scisignal.2004088.
65. Szklarczyk D, Gable AL, Lyon D, Junge A, Wyder S, Huerta-Cepas J, Simonovic M, Doncheva NT, Morris JH, Bork P, et al. (2019). STRING v11: protein-protein association networks with increased coverage, supporting functional discovery in genome-wide experimental datasets. Nucleic Acids Res. 47, D607–D613. 10.1093/nar/gky1131. [PubMed: 30476243]

66. Bolger AM, Lohse M, and Usadel B. (2014). Trimmomatic: a flexibletrimmer for Illumina sequence data. Bioinformatics 30, 2114–2120. 10.1093/bioinformatics/btu170. [PubMed: 24695404]

67. Dobin A, Davis CA, Schlesinger F, Drenkow J, Zaleski C, Jha S,Batut P, Chaisson M, and Gingeras TR (2013). STAR: ultrafast universal RNA-seq aligner. Bioinformatics 29, 15–21. 10.1093/bioinformatics/bts635. [PubMed: 23104886]

68. Love MI, Huber W, and Anders S. (2014). Moderated estimation of foldchange and dispersion for RNA-seq data with DESeq2. Genome Biol. 15, 550. 10.1186/s13059-014-0550-8. [PubMed: 25516281]

69. Luo W, Friedman MS, Shedden K, Hankenson KD, and Woolf PJ(2009). GAGE: generally applicable gene set enrichment for pathway analysis. BMC Bioinf. 10, 161. 10.1186/1471-2105-10-161.

70. Gao S, Zhang Y, Yang C, Perez GI, and Xiao H. (2019). NCOA5 Haplo-insufficiency Results in Male Mouse Infertility through Increased IL-6 Expression in the Epididymis. Sci. Rep. 9, 15525. 10.1038/s41598-019-52105-9. [PubMed: 31664153]

71. Borowicz S, Van Scoyk M, Avasarala S, Karuppusamy Rathinam MK, Tauler J, Bikkavilli RK, and Winn RA (2014). The soft agar colony formation assay. J. Vis. Exp. e51998. 10.3791/51998.

Highlights

- *Tip30* heterozygous deletion increases HCC rate in *Ncoa5*$^{+/-}$mice in a female-biased manner
- HCN3 is preferentially upregulated in the liver of dual *Tip30* and *Ncoa5* mutant female mice
- HCN3 has female-biased oncogenic activities to promote HCC development
- *HCN3* overexpression correlates with poor prognosis of HCC patients with a female bias

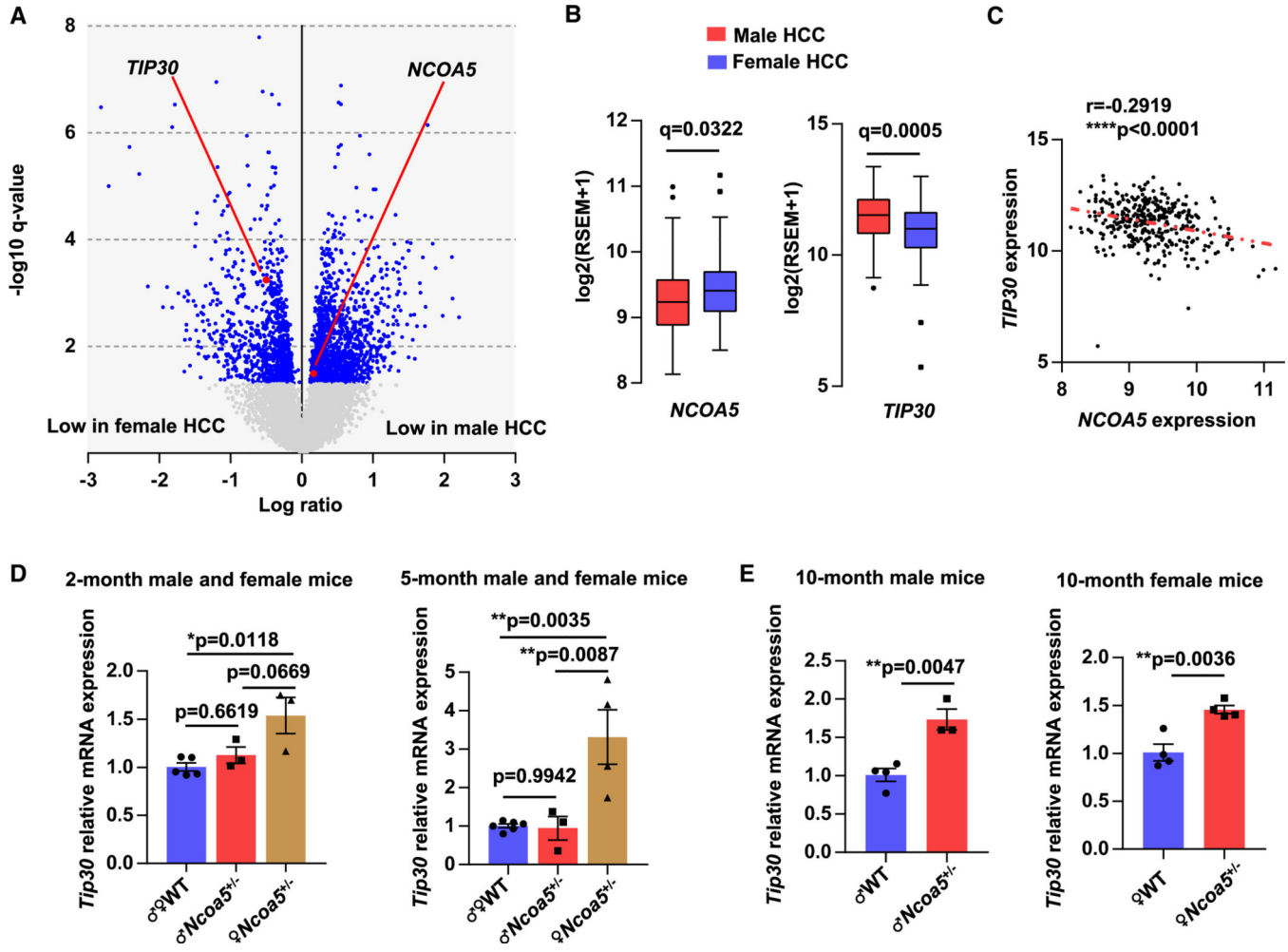

Figure 1. Gene expression differences between male and female HCC samples from the TCGA cohort and the correlation between NCOA5 and TIP30 expression in humans and mice

(A) Volcano plot showing differentially expressed genes (DEGs) between primary HCC samples from male (n = 244) and female (n = 117) patients in the TCGA cohort. Welch's t test with the false discovery rate (FDR) method of Benjamini-Hochberg. q cutoff at 0.05. Genes on XY chromosomes are not included in the graph.

(B) Box plots (Tukey method) showing mRNA levels of NCOA5 and TIP30 in male and female primary HCC samples. q values from the result shown in (A).

(C) Correlation between NCOA5 and TIP30 mRNA levels in primary HCC samples from male and female patients in the TCGA cohort. n = 361. Pearson correlation.

(D) qRT-PCR analysis of the *Tip30* mRNA levels in the livers of mice. Left: 2-month-old wild-type (WT) male (n = 3) and female (n = 2) mice, and *Ncoa5*$^{+/-}$ male (n = 3) and female mice (n = 3). Right: 5-month-old WT male (n = 4) and female (n = 2) mice, and *Ncoa5*$^{+/-}$ male (n = 3) and female (n = 4) mice. One-way ANOVA, Tukey's multiple comparison test.

(E) qRT-PCR analysis of the *Tip30* mRNA levels in 10-month-old WT (n = 4) and *Ncoa5*$^{+/-}$ (n = 3) male mice (left) and 10-month-old WT (n = 4) and *Ncoa5*$^{+/-}$ (n = 4) male mice (right). Two-tailed unpaired Student's t test.

Data are presented as mean ± SEM. ****p < 0.0001, **p < 0.01, *p < 0.05. See also Figure S1.

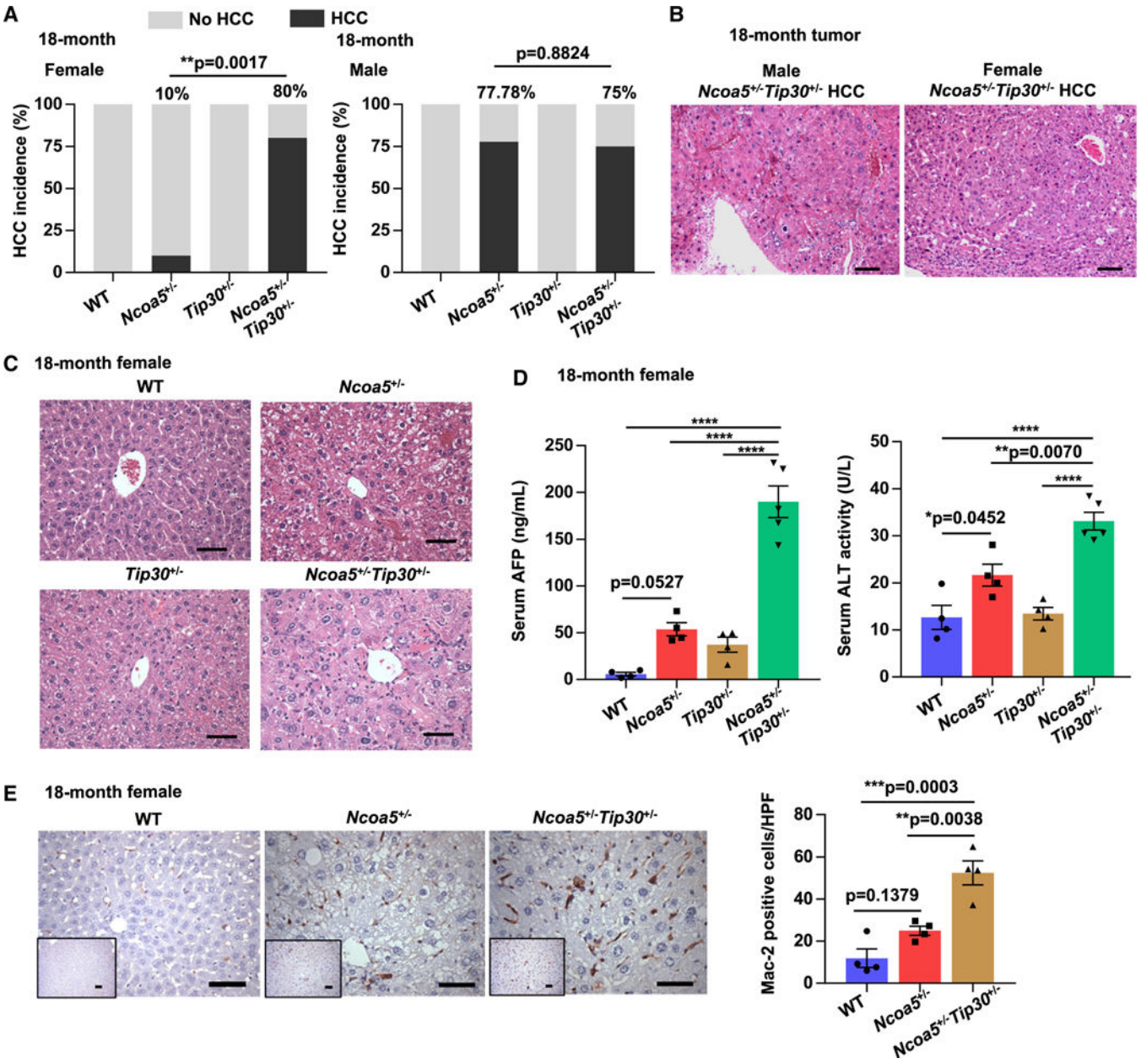

Figure 2. HCC incidence and histopathology features in 18-month-old male and female mice with *Ncoa5* and/or *Tip30* deficiency

(A) HCC incidence in 18-month-old female and male mice with indicated genotype. Female mice (left) n = 12, 10, 15, or 10; male mice (right) n = 6, 9, 11, or 12. Chi-squared test, **p < 0.01.

(B) Representative H&E-staining photos of moderately differentiated HCCs from *Ncoa5*$^{+/-}$*Tip30*$^{+/-}$ male or female mice. Grading was according to the WHO classification.[35] Scale bars, 100 μm.

(C) Representative H&E-staining photos of non-tumor adjacent liver from 18-month-old female mice as indicated. See Figure S1C for histological features scored according to the Modified Hepatic Activity Index system.[36] Scale bars, 50 μm.

(D) Serum AFP level and ALT activity in 18-month-old female mice (n = 4 per group) as indicated. One-way ANOVA, Tukey's multiple comparison test.
(E) Representative Mac-2 IHC staining photos and analysis of livers from 18-month-old female mice (n = 4 per group) as indicated. One-way ANOVA, Tukey's multiple comparison test. Scale bars, 50 μm.
Data are presented as mean ± SEM. ****p < 0.0001, ***p < 0.001, **p < 0.01, *p < 0.05.
See also Figure S1.

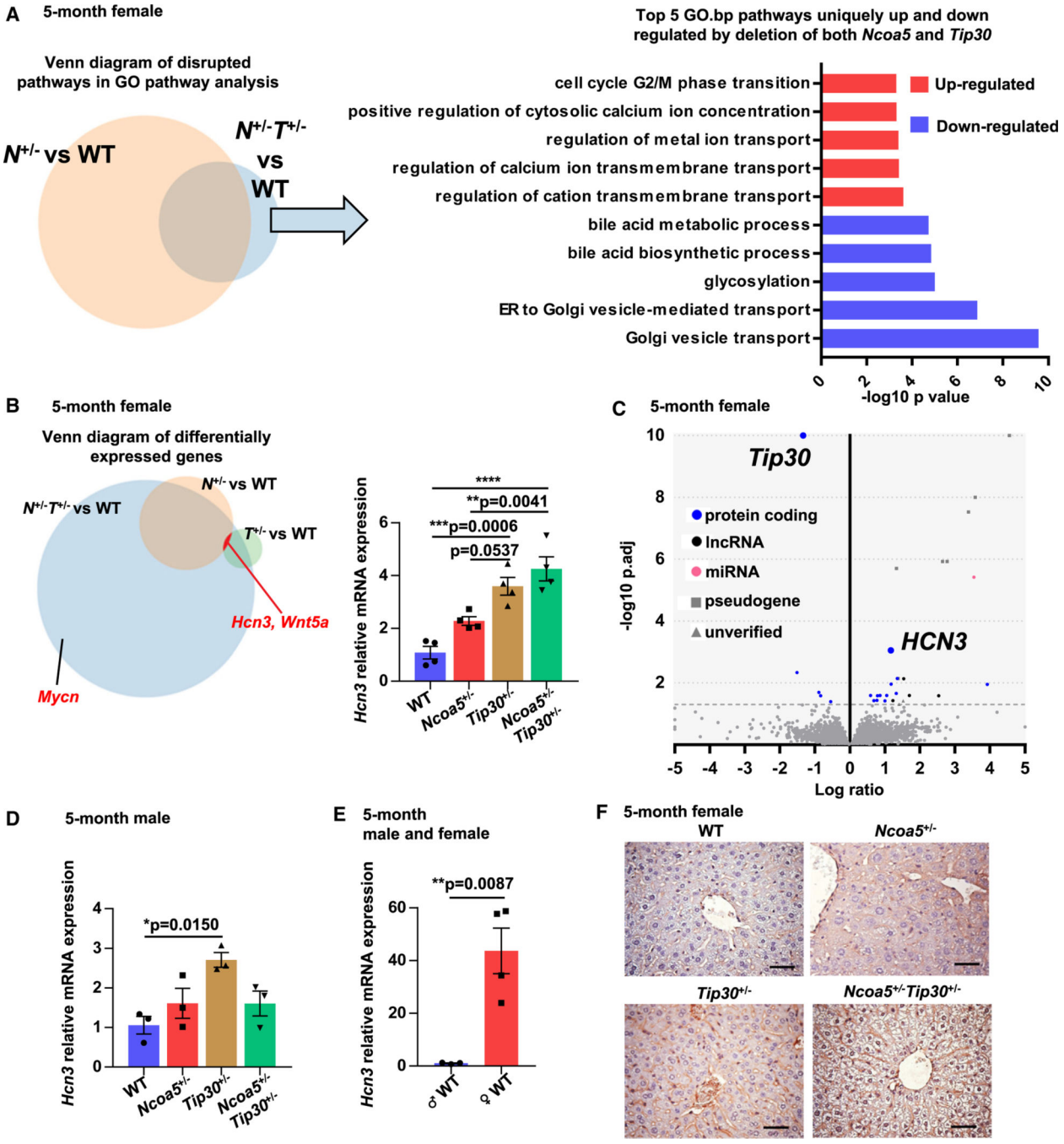

Figure 3. Transcriptome analysis of livers of 5-month-old wild-type, *Ncoa5*$^{+/-}$, *Tip30*$^{+/-}$, and *Ncoa5*$^{+/-}$*Tip30*$^{+/-}$ female mice and the expression of HCN3 in male and female mice

(A) Disrupted pathways in GO.bp pathway analyses comparing liver transcriptomes of *Ncoa5*$^{+/-}$ or *Ncoa5*$^{+/-}$ *Tip30*$^{+/-}$ female mice vs. wild-type (WT) female mice. n = 4 in each group. Left: Venn diagram. Pathways with q < 0.05 were recognized as significantly disrupted pathways. Right: top five GO.bp pathways uniquely up- and downregulated by deletion of both *Ncoa5* and *Tip30*, but not by deletion of *Ncoa5* or *Tip30* alone.

(B) DEGs between liver transcriptomes of *Ncoa5*$^{+/-}$, *Tip30*$^{+/-}$, or *Ncoa5*$^{+/-}$ *Tip30*$^{+/-}$ female mice and WT female mice. n = 4 in each group. Left: Venn diagram. Right: qRT-PCR

analysis of the mRNA levels of identified commonly upregulated gene *Hcn3* in livers of 5-month-old female mice (n = 4 per group) as indicated. One-way ANOVA, Tukey's multiple comparison test.

(C) Volcano plot showing DEGs between livers of 5-month-old *Ncoa5*$^{+/-}$ and *Ncoa5*$^{+/-}$ *Tip30*$^{+/-}$ female mice and their gene classes. DEGs with adjusted $p < 0.05$ were recognized as significant. —Log_{10} p_{adj} values larger than 10 were drawn as 10, and log_2 fold-change values larger than 5 were drawn as 5.

(D) qRT-PCR analysis of *Hcn3* mRNA levels in livers of 5-month-old male mice (n = 3 per group). One-way ANOVA, Tukey's multiple comparison test.

(E) qRT-PCR analysis of *Hcn3* mRNA levels in livers of 5-month-old male and female WT mice (n = 3 or 4). Two-tailed unpaired Student's t test.

(F) Representative HCN3 IHC in livers of 5-month-old female mice (n = 3 per group). Staining scores according to the immunoreactive score (IRS) system[39,40] are shown in Figure S3G. Scale bars, 50 μm.

Data are presented as mean ± SEM. ****$p < 0.0001$, ***$p < 0.001$, **$p < 0.01$, *$p < 0.05$. See also Figures S2 and S3.

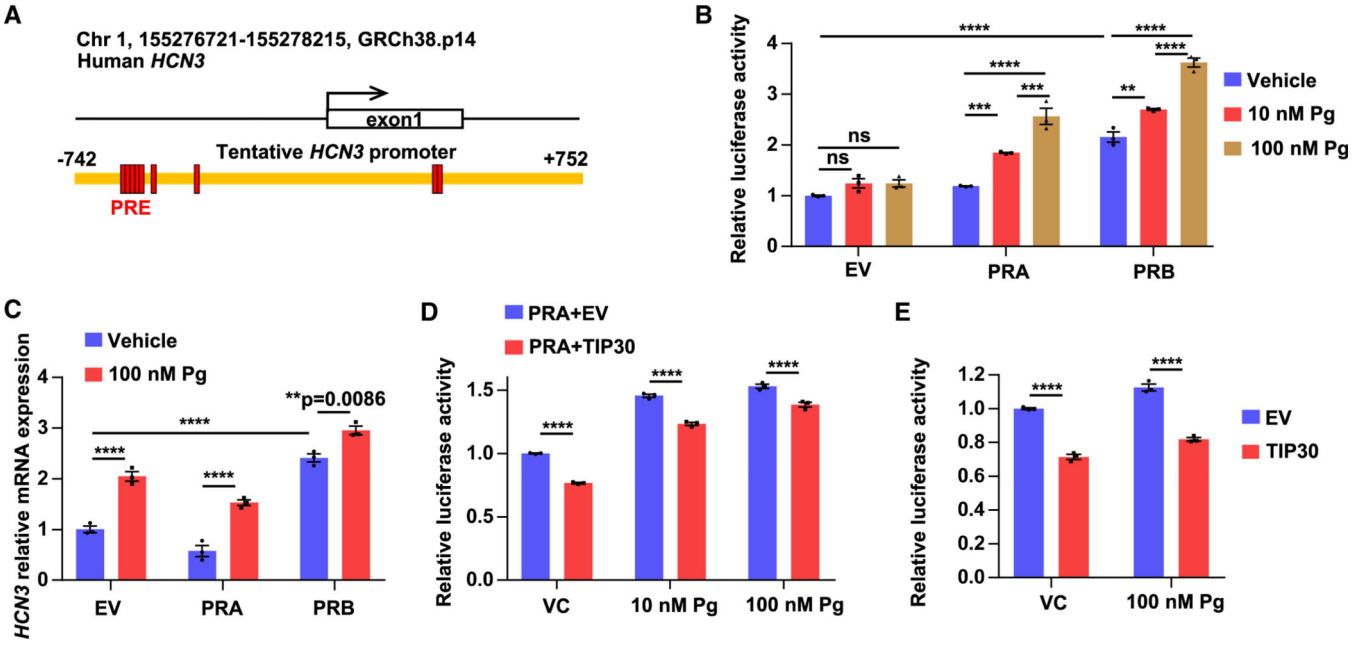

Figure 4. Transcriptional regulation of *HCN3* by Pg and PRs

(A) Diagram of the putative promoter region of human *HCN3* and the relative locations of predicted PREs in the HCN3 promoter-luciferase reporter plasmid.

(B) Relative luciferase activity of the *HCN3* promoter in PLC/PRF/5 HCC cells transfected with empty vector (EV), PRA-expressing vector, or PRB-expressing vector with or without Pg treatment. Two-way ANOVA, Tukey's multiple comparisons test.

(C) qRT-PCR analysis of *HCN3* mRNA levels in PLC/PRF/5 cells transfected with EV, PRA-expressing vector, or PRB-expressing vector with or without Pg- treatment. Two-way ANOVA, Tukey's multiple comparisons test.

(D) Relative luciferase activity of the *HCN3* promoter in PLC/PRF/5 cells transfected with PRA-expressing vector together with EV or TIP30-expressing vector with or without Pg treatment. VC, vehicle control. Two-way ANOVA, Sidak's multiple comparison test.

(E) Relative luciferase activity of the *HCN3* promoter in PLC/PRF/5 cells transfected with EV or TIP30-expressing vector with or without Pg treatment. Two-way ANOVA, Sidak's multiple comparison test.

Representative data of three repeats. Data are presented as mean ± SEM. ****p < 0.0001, ***p < 0.001, **p < 0.01. See also Figure S4.

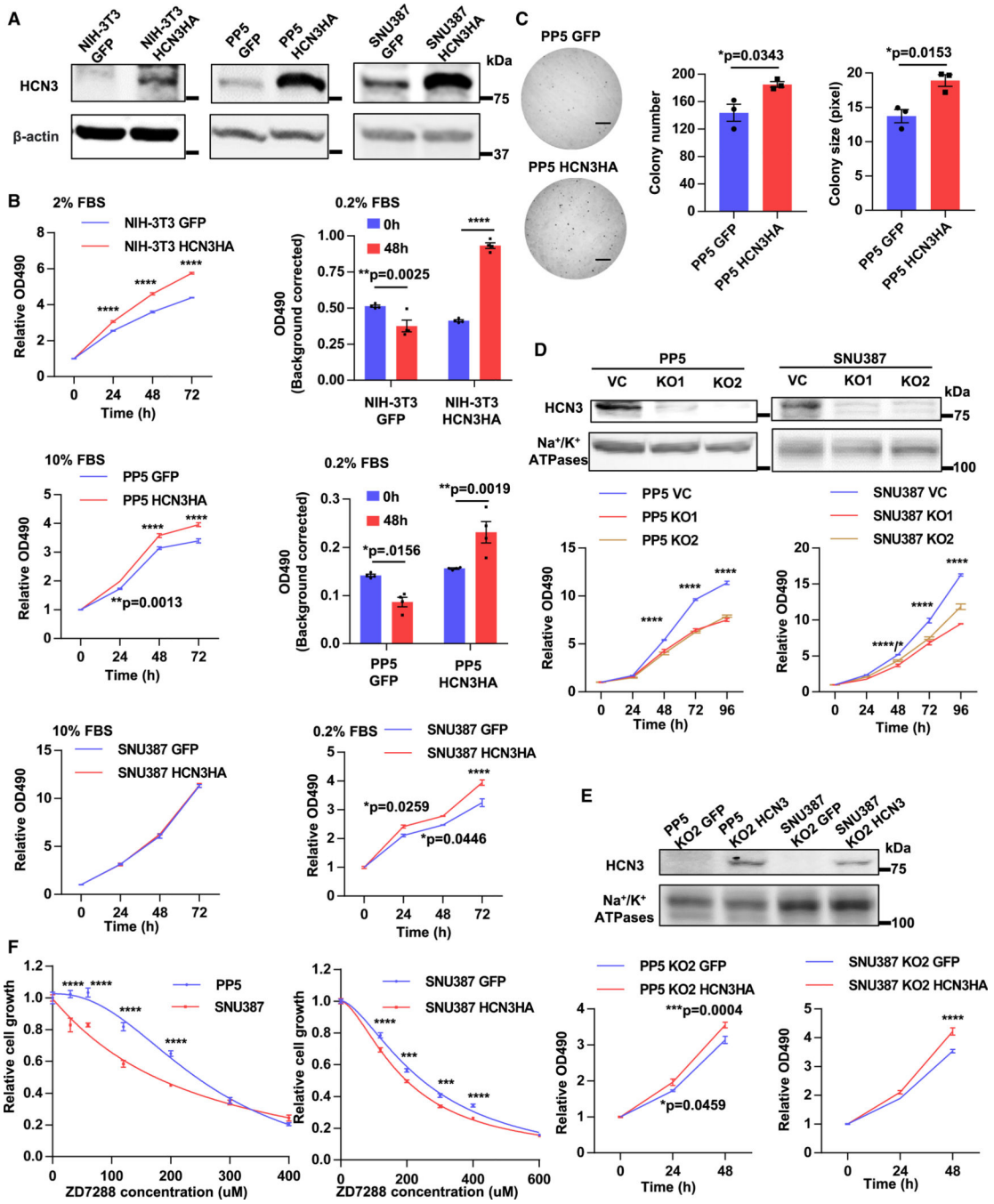

Figure 5. Effects of HCN3 overexpression, knockout, or inhibition on cell proliferation and survival *in vitro*

(A) Western blot of HCN3 overexpression in cell lines as indicated.

(B) Effect of HCN3 overexpression on cell proliferation of NIH-3T3 (top), PLC/PRF/5 (PP5) (middle), and SNU-387 (bottom) cells. Cells were grown in a medium supplemented with fetal bovine serum (FBS) in concentration as indicated. Two-way ANOVA, Sidak's multiple comparison test.

(C) Representative photos and soft agar colony-formation assays on PLC/PRF/5 cells with or without HCN3 overexpression. Two-tailed unpaired Student's t test. Scale bar, 2.5 mm.

(D) Effect of HCN3 knockout on cell proliferation. Western blot validation of HCN3 CRISPR knockout in cell lines as indicated. VC, vector control. Cells were grown in medium with 10% FBS. Two independent single clones for each cell line were analyzed. Two-way ANOVA, Sidak's multiple comparison test.

(E) Effect of HCN3 compensation on cell proliferation of HCN3 knockout cells. Top: western blot of HCN3 compensation in HCN3 knockout cells as indicated. Bottom: proliferation of HCN3 knockout cells with HCN3 compensation. two-way ANOVA, Sidak's multiple comparison test.

(F) Effect of HCN inhibition by ZD7288 on the growth of cell lines as indicated. Two-way ANOVA, Sidak's multiple comparison test.

Representative data of three repeats. Data are presented as mean ± SEM. ****$p < 0.0001$, ***$p < 0.001$, **$p < 0.01$, *$p < 0.05$. See also Figure S4.

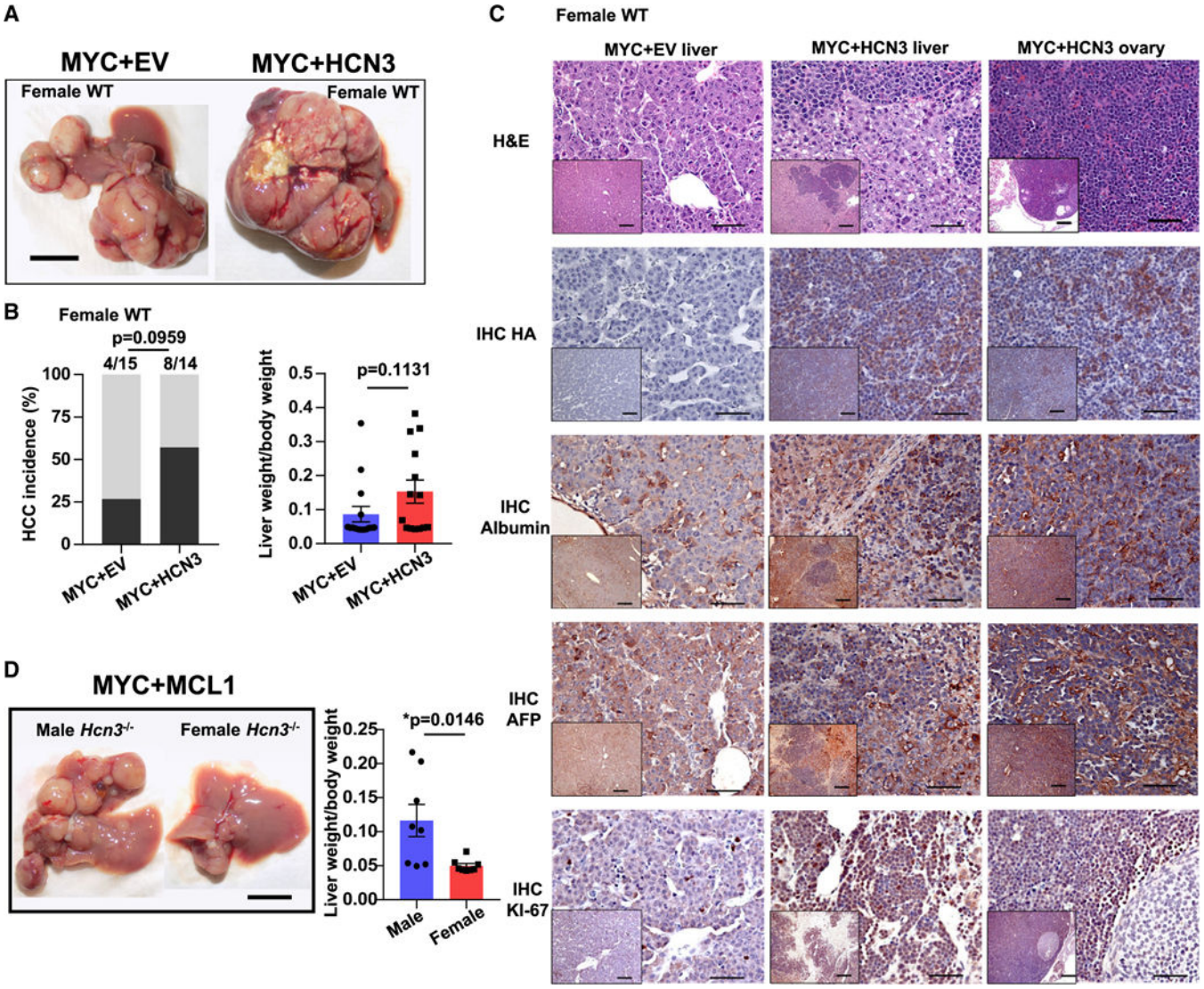

Figure 6. Formation of liver tumors induced by overexpression of *MYC* and *HCN3* in wild-type female mice and by overexpression of *MYC* and *MCL1* in *Hcn3*$^{-/-}$ mice

(A) Representative macroscopic photos of liver tumor formed in wild-type (WT) female mice injected with MYC-expressing vector + empty vector (EV) (n = 14) or MYC + HCN3-expressing vectors (n = 15). Scale bar, 1 cm.

(B) Liver tumor incidence and liver/body weight ratio of WT female mice injected with MYC + EV or MYC + HCN3-expressing vectors. Chi-squared test and two-tailed unpaired Student's t test.

(C) Representative H&E staining and IHC for hemagglutinin (HA) that tags HCN3, IHC for hepatocyte marker albumin and AFP, and IHC for the proliferation marker Ki-67 in MYC-induced and MYC + HCN3-induced HCCs in female mice. Staining scores according to the IRS system can be found in Figure S4F. Scale bars, 50 μm and 100 μm (insets).

(D) Representative macroscopic photos and analysis of liver/body weight ratio of *Hcn3*$^{-/-}$ male and female mice (n = 8 per group) injected with MYC + MCL1 vectors. Scale bar, 1 cm. Two-tailed unpaired Student's t test.

Data are presented as mean ± SEM. *p < 0.05. See also Figure S4.

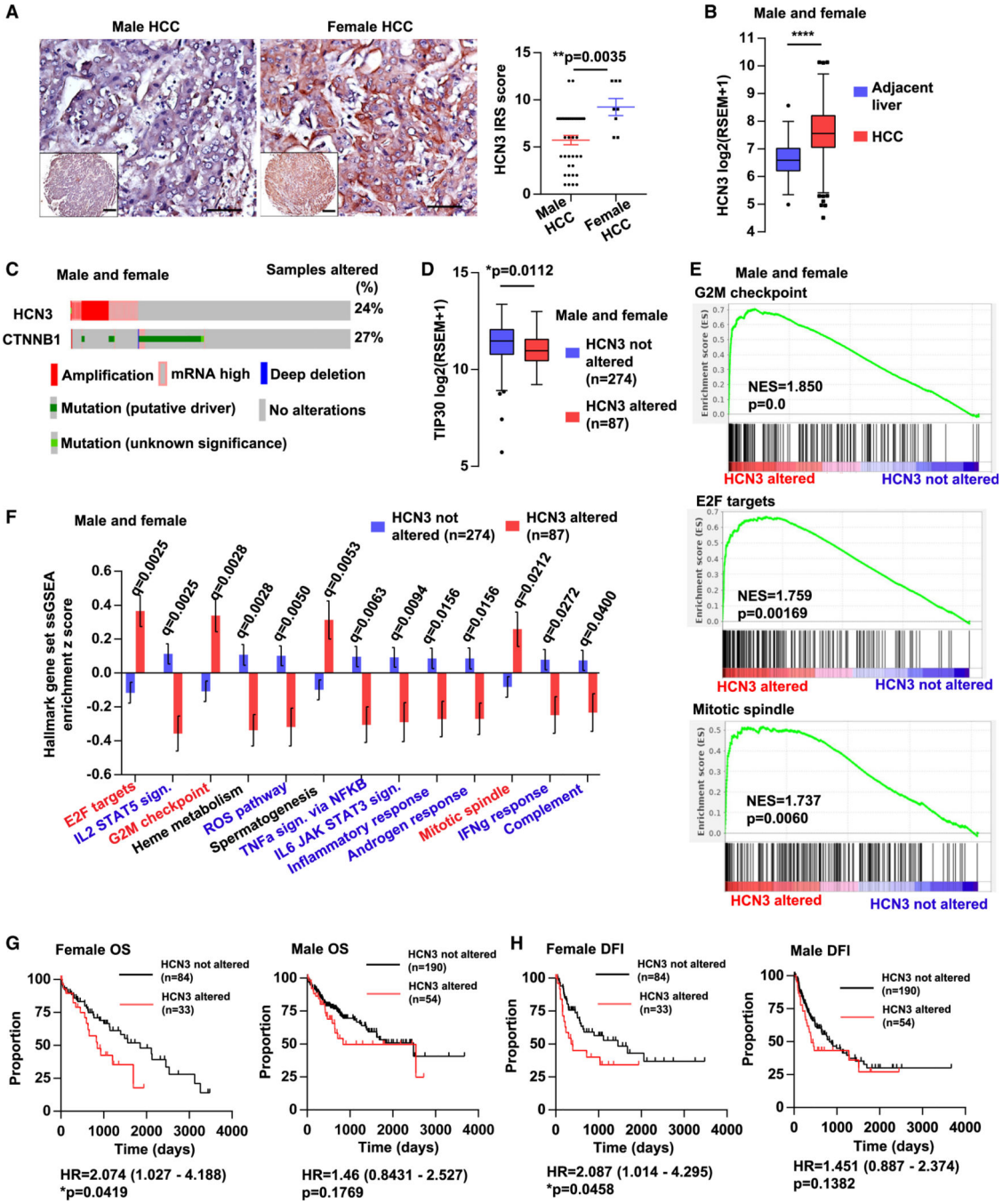

Figure 7. HCN3 expression and copy-number variation in TCGA HCC patients and their relationship with prognosis and hallmark pathway enrichment

(A) Representative IHC staining photos and analysis of staining score of HCN3 in primary HCCs from male (n = 38) and female (n = 8) patients. HCN3 staining was scored according to the IRS system. Scale bars: 50 μm and 200 μm (insets). Mann-Whitney U test.

(B) mRNA expression of *HCN3* in adjacent non-tumor livers (n = 49) and primary HCCs (n = 361) from the TCGA cohort. Two-tailed unpaired Welch's t test. Box plot was drawn using the Tukey method.

(C) Genetic alterations and gene expression change relative to diploid samples of *HCN3* and *CTNNB1* in primary HCC samples of TCGA cohorts. Samples with gene mRNA expression *Z* score >3 or <—3 were recognized as having high or low expression.
(D) mRNA expression of *TIP30* in primary HCC samples without (n = 274) or with (n = 87) HCN3 amplification and/or overexpression (regarded as HCN3 alterations) in the TCGA cohort. Two-tailed unpaired Welch's t test. Box plot was drawn using the Tukey method.
(E) GSEA result showing significantly differentially enriched hallmark pathways (FDR < 0.1) between the transcriptome of HCCs with and without HCN3 alterations (n = 87 or n = 274). Normalized enrichment score and p value are shown.
(F) ssGSEA enrichment score of hallmark pathways in primary HCC samples with or without HCN3 alterations (n = 87 or n = 274). Welch's t test with two-stage step-up FDR method for 52 comparisons. Pathways with q < 0.05 were recognized as significantly different and shown.
(G and H) Kaplan-Meier plots of overall survival (OS) (G) and disease-free survival/interval (DFI) (H) of female (left) or male (right) patients with or without HCN3 alterations. Curated survival data.[52] DFI: the period from the date of diagnosis until the date of the first new tumor progression event subsequent to the determination of a patient's disease-free status after their initial diagnosis and treatment.[52] Log-rank test, hazard ratio calculated using the Mantel-Haenszel method.
Data are presented as mean ± SEM. ****p < 0.0001, **p < 0.01, *p < 0.05. See also Figures S5–S7 and Tables S1–S3.

KEY RESOURCES TABLE

REAGENT or RESOURCE	SOURCE	IDENTIFIER
Antibodies		
Anti Mac-2 (Galectin-3)	Cedarlane Labs	Cat#CL8942AP; RRID:AB_10060357
Anti IL-6	Santa Cruz Biotechnology	Cat#sc-1265; RRID:AB_2127470
Anti Na^+/K^+-ATPases	Santa Cruz Biotechnology	Cat#sc-48345; RRID:AB_626712
Anti β-Actin	Santa Cruz Biotechnology	Cat#sc-47778; RRID:AB_626632
Anti HCN3	Abcam	Cat#ab84818; RRID:AB_1861081
Anti HCN3	Alomone Labs	Cat#APC-057; RRID:AB_2039904
Anti HCN3	Thermo Fisher	Cat#MA3-902; RRID:AB_2115028
Anti HA-tag	Cell Signaling Technology	Cat#3724; RRID:AB_1549585
Anti AFP	Proteintech	Cat#14550-1-AP; RRID:AB_2223933
Anti Albumin	Proteintech	Cat#16475-1-AP; RRID:AB_2242567
Anti Ki-67	Millipore-Sigma	Cat#AB9260; RRID:AB_2142366
Anti NCOA5	Bethyl	Cat#A300-790A; RRID:AB_2151214
Anti TIP30	Xiao lab (Ito et al.)[28]	N/A
Anti PR	Cell Signaling Technology	Cat#8757; RRID:AB_2797144
LICOR IRDye 800CW secondary antibodies	LICOR	Cat#923-32213, 926-32214, 926-32211
LICOR IRDye 680RD secondary antibodies	LICOR	Cat#926-68072, 925-68074, 925-68076
Bacterial and virus strains		
E. coli DH5α	Thermo Fisher	Cat#EC0112
E. coli TOP10	Thermo Fisher	Cat#C404010
Biological samples		
Human HCC tissue array	TissueArray.Com LLC	Cat#LV1505a
Chemicals, peptides, and recombinant proteins		
RIPA Lysis and Extraction Buffer	Thermo Fisher	Cat#89900
Formalin solution, neutral buffered, 10%	Sigma-Aldrich	Cat#HT501128
TRIzol Reagent	Thermo Fisher	Cat#15596026
PowerUp SYBR Green reagent	Thermo Fisher	Cat#A25742
Lipofectamine 3000	Thermo Fisher	Cat#L3000015
QuickExtract DNA Extraction Solution	Lucigen	Cat#QE0905T
SuperScript IV First-Strand Synthesis System	Thermo Fisher	Cat#18091050
(R)-MG132	Cayman Chemical	Cat#13697
ZD7288	Tocris	Cat#1000
Polyethyleneimine	Polysciences, Inc.	Cat#23966-1
Puromycin dihydrochloride	Thermo Fisher	Cat#A1113803
Nitrotetrazolium Blue chloride	Sigma-Aldrich	Cat#N6639
Laemmli Sample Buffer	BIO-RAD	Cat#1610747

REAGENT or RESOURCE	SOURCE	IDENTIFIER
Thapsigargin	Millipore-Sigma	Cat#586005
Critical commercial assays		
Biorad Protein Assay	BIO-RAD	Cat#5000006
VECTASTAIN Elite ABC-HRP system	Vector Laboratories	Cat#PK-6101, PK-6102
Cell Counting Kit-8	Dojindo	Cat#CK04
Alanine Transaminase Colorimetric Activity Assay	Cayman Chemical	Cat#700260
Mouse AFP Quantikine ELISA Kit	R&D Systems	Cat#MAFP00
Dual-Luciferase Reporter Assay System	Promega	Cat#E1910
Mouse IL-6 ELISA Kit	Proteintech	Cat#KE10007
Deposited data		
Raw and processed RNA sequencing data	This study	GEO: GSE228531
Experimental models: Cell lines		
NIH/3T3	ATCC	Cat#CRL-1658; RRID:CVCL_0594
HEK293T	ATCC	Cat#CRL-3216; RRID:CVCL_0063
PLC/PRF/5	ATCC	Cat#CRL-8024; RRID:CVCL_0485
SNU-387	ATCC	Cat#CRL-2237; RRID:CVCL_0250
Experimental models: Organisms/strains		
Mouse: *Ncoa5*$^{+/-}$ BALB/c	Xiao lab (Gao et al.)[8]	N/A
Mouse: *Tip30*$^{+/-}$ BALB/c	Xiao lab (Ito et al.)[28]	N/A
Mouse: *Ncoa5*$^{+/-}$ *Tip30*$^{+/-}$ BALB/c	This study	N/A
Mouse: *Hcn3*$^{-/-}$ C57BL/6	Biel lab (Fenske et al.)[49]	N/A
Mouse: *Hcn3*$^{-/-}$ BALB/c	This study	N/A
Mouse: BALB/cJ	Jackson Laboratory	Cat#000651; RRID:IMSR_JAX:000651
Oligonucleotides		
See Table S4 for PCR primer sequences	N/A	N/A
Recombinant DNA		
HCN3 CDS containing plasmid	DF/HCC DNA Resource Core	HsCD00348243
pSin-EF2 vector	Yu et al.[58]	Addgene Cat#16579; RRID:Addgene_16579
pSpCas9(BB)-2A-Puro (PX459) V2.0	Ran et al.[59]	Addgene Cat#62988; RRID:Addgene_62988
pCMV delta R8.2	Trono Lab Packaging and Envelope Plasmids (unpublished)	Addgene Cat#12263; RRID:Addgene_12263
pMD2.G	Trono Lab Packaging and Envelope Plasmids (unpublished)	Addgene Cat#12259; RRID:Addgene_12259
pGL2-Basic	Promega	N/A
pcDNA3-TIP30	Xiao lab (Zhang et al.)[60]	N/A

REAGENT or RESOURCE	SOURCE	IDENTIFIER
pcDNA3-hPR-A	Su et al.[61]	Addgene Cat#89119; RRID:Addgene_189119
pcDNA3-PRB	Su et al.[61]	Addgene Cat#89130; RRID:Addgene_89130
pRL	Promega	N/A
pT3-EF1α-c-MYC	Chen lab (Mendez-Lucas et al.)[48]	N/A
pT3-EF1α-MCL1	Chen lab (Mendez-Lucas et al.)[48]	N/A
pCMV/SB	Chen lab (Mendez-Lucas et al.)[48]	N/A
pSin-EF2-HCN3HA	This study	N/A
PX459V2-HCN3-T1	This study	N/A
PX459V2-HCN3-T2	This study	N/A
pGL2-promoHCN3	This study	N/A
pT3-EF1α empty vector	This study	N/A
pT3-EF1α-HCN3HA	This study	N/A
Software and algorithms		
UCSC Xena	Goldman et al.[62]	https://xena.ucsc.edu/
cBioportal	Cerami et al.[63]; Gao et al.[64]	https://www.cbioportal.org/
STRING	Szklarczyk et al.[65]	https://string-db.org/
Gene Set Enrichment Analysis	Subramanian et al.[51]	https://www.gsea-msigdb.org/gsea/index.jsp
ssGSEA	Barbie et al.[50]	https://gsea-msigdb.github.io/ssGSEA-gpmodule/v10/index.html
Trimmomatic	Bolger et al.[66]	http://www.usadellab.org/cms/?page=trimmomatic
STAR	Dobin et al.[67]	https://github.com/alexdobin/STAR
DESeq2	Love et al.[68]	https://bioconductor.org/packages/release/bioc/html/DESeq2.html
GAGE	Luo et al.[69]	https://bioconductor.org/packages/release/bioc/html/gage.html
GraphPad Prism	GraphPad Software	https://www.graphpad.com/